Synthesis, Structural Characterisation and Studies of Octanuclear Copper Complexes of Pyridonate and Carboxylate Ligands†

Alexander J. Blake,[a] Craig M. Grant,[a] Christopher I. Gregory,[b] Simon Parsons,[a] Jeremy M. Rawson,[a] David Reed[a] and Richard E. P. Winpenny*,[a]
[a] *Department of Chemistry, The University of Edinburgh, West Mains Road, Edinburgh EH9 3JJ, UK*
[b] *Department of Physics, University of Durham, South Road, Durham DH1 3LE, UK*

A series of octanuclear copper(II) complexes has been prepared which features carboxylate and 2-pyridonate ligands. These compounds have the general formula $[Cu_8(O)_2(O_2CR)_4L_8]$ (where R = Me, Ph or CF_3, and L = 6-chloro-, 6-bromo- or 6-methyl-2-pyridonate). X-Ray structural analyses of the acetate complexes indicate that the compounds contain an edge-sharing Cu_6O_2 bitetrahedral core, surrounded by two $[CuL_4]$ units. The Cu$\cdots$Cu contacts within the core vary from 2.92 to 3.58 Å, depending on the ligand bridging the metal–metal vector. Two routes to these complexes have been investigated, one involving reaction of preformed copper pyridonate complexes with copper carboxylates, the second involving reaction of copper carboxylates with molten HL. Differential scanning calorimetry and thermogravimetric analysis studies of the latter route show it proceeds *via* formation of copper pyridonate complexes. The FAB mass spectral results show interesting fragmentation patterns, consistent with the observed structures, and NMR spectra of the octanuclear complexes show paramagnetically shifted resonances due to both the pyridonate and carboxylate ligands. Magnetic studies of $[Cu_8(O)_2(O_2CMe)_4L_8]$ (L = 6-chloro- or 6-bromo-2-pyridonate) show largely antiferromagnetic exchange coupling within the Cu_6O_2 core. The structure of the complexes and the magnitude of the couplings lead to spin-frustrated systems, with subtle differences between the two complexes studied.

Although polynuclear copper complexes are well known and have been studied for a number of years, the vast majority of such compounds contain copper in the +1 oxidation state.[1] For the +2 oxidation state compounds which contain up to six metal atoms are not rare,[2–15] but compounds with seven,[16,17] eight[18–21] or more[15,22–25] copper(II) atoms remain comparatively unusual. We have been investigating the ability of ligands derived from 2-pyridone (2-hydroxypyridine) to stabilise polynuclear assemblies. As part of this work we have reported the synthesis of a dinuclear copper complex $[Cu_2(chp)_4]$ **1**[26] and the novel hexa- and hepta-nuclear complexes $[Cu_6Na(mhp)_{12}][NO_3]$ **2**[15] and $[Cu_7(mhp)_{12}][Pb(NO_3)_4]$[16] (chp = 6-chloro-2-pyridonate, mhp = 6-methyl-2-pyridonate). Here we report the reactions of both **1** and **2** with dimeric copper carboxylates, which lead to new octanuclear copper complexes featuring an unusual edge-sharing oxo-centred bitetrahedral core. A preliminary report of a portion of this work has appeared.[27]

Experimental

The compounds $[Cu_2(chp)_4]$ **1** and $[Cu_6Na(mhp)_{12}][NO_3]$ **2** were prepared as described previously;[15,26] $[Cu_2(bhp)_4]$ **3** was prepared by a directly analogous procedure (bhp = 6-bromo-2-pyridonate).[28] Hydrated copper acetate was obtained from Fisons. Copper benzoate was prepared by reaction of $Cu(NO_3)_2{\cdot}3H_2O$ with sodium benzoate in water; the resultant pale blue precipitate was washed with ethanol and diethyl ether and dried *in vacuo*. Copper trifluoroacetate was prepared by the reaction of freshly prepared copper hydroxide with trifluoroacetic acid in water. The pyridone derivatives Hmhp and Hchp were obtained from Aldrich and used without further purification; Hbhp was synthesised by a published procedure.[29] All solvents were used as obtained. Analytical data and yields for compounds **4** and **6**–**9** are given in Table 1.

The NMR spectra were recorded on a Bruker AM-360 MHz spectrometer in $CDCl_3$. Mass spectra were obtained using both fast-atom bombardment and electron impact on samples in a 3-nitrobenzyl alcohol matrix. The EPR spectroscopy was attempted on a Bruker ER200D-SRC spectrometer operating at X-band frequency; however all compounds were EPR silent as solutions (CH_2Cl_2, 298), as frozen solutions (CH_2Cl_2, 77) and as powders (298 K). Thermogravimetric analysis (TGA) studies were carried out on a Stanton Redcroft TG770 instrument at a heating rate of 2 °C min^{-1} and differential scanning calorimetry (DSC) studies on a Mettler FP85 thermal analysis cell, coupled to a Mettler FP80 processing unit. Samples were hermetically sealed in aluminium capsules and heating was performed under argon. Data collection and manipulation were carried out on an OPUS PCIII using in-house software.[30]

Preparation of Compounds **4**–**10**.—$[Cu_8(O)_2(O_2CMe)_4(chp)_8]$ **4**. *Route* (*a*). Compound **1** (0.641 g, 1 mmol) was dissolved in CH_2Cl_2 (15 cm^3) and filtered onto an excess of hydrated copper acetate, $[Cu_2(O_2CMe)_4(H_2O)_2]$ (1.6 g, 4 mmol) and stirred for 4 h. During this time the initially red solution became dark green. The solution was filtered to remove unreacted copper acetate. Diethyl ether vapour was allowed to diffuse into the filtrate, leading to the formation of dark green crystals of **4** over a period of 18–36 h.

Route (*b*). Hydrated copper acetate (3.99 g, 10 mmol) and a slightly greater than two-fold equivalent of Hchp (2.85 g, 22 mmol) were ground together to form an intimate mixture

---

† *Supplementary data available:* see Instructions for Authors, *J. Chem. Soc., Dalton Trans.*, 1995, Issue 1, pp. xxv–xxx.

Non-SI units employed: emu = SI × $10^6/4\pi$, $\mu_B = 9.27 \times 10^{-24}$ J T^{-1}.

Table 1 Analytical data[a] for compounds **4** and **6**–**10**

Compound	Formula	Analysis (%) C	H	N	Yield (%) Route A	Route B
4	$Cu_8(O)_2(chp)_8(O_2CMe)_4$	32.3 (31.9)	2.1 (2.0)	6.1 (6.2)	78	62
6	$Cu_8(O)_2(bhp)_8(O_2CMe)_4$	27.2 (26.7)	1.8 (1.7)	5.2 (5.2)	65	60
7	$Cu_8(O)_2(chp)_8(O_2CPh)_4$	37.2 (36.9)	2.1 (2.2)	4.9 (4.9)	59	*b*
8	$Cu_8(O)_2(bhp)_8(O_2CPh)_4$	34.0 (33.9)	1.9 (1.8)	5.0 (4.7)	62	*b*
9	$Cu_8(O)_2(chp)_8(O_2CCF_3)_4$	28.5 (28.4)	1.2 (1.2)	5.6 (5.4)	76	*b*
10	$Cu_2(mhp)_4$	53.5 (51.5)	4.9 (4.3)	10.1 (10.0)	*c*	89

[a] Calculated values are given in parentheses. [b] Not attempted. [c] Not applicable.

which was heated to 130 °C, causing the Hchp to melt. During this time the reaction mixture became deep red, indicative of the formation of **1**. After 30 min the acetic acid formed during the reaction was removed by distillation under reduced pressure. Unreacted Hchp was also removed by sublimation, leaving a dark green residue. Addition of CH_2Cl_2 (50 cm^3) initially gave a deep red solution which within minutes turned green. This solution was subsequently filtered, before crystallisation by diffusion of ether vapour into the solution. Both routes led to samples which gave identical analytical data (see Table 1). The NMR data are given in Table 10. FAB mass spectrum (significant peaks, possible assignments): *m*/*z* 1173, $[Cu_6(O)_2(O_2CMe)_2(chp)_5]$; 986, $[Cu_6(O)_2(O_2CMe)(chp)_4]$; 919, $[Cu_6(O)_2(O_2CMe)_2(chp)_3]$; 858, $[Cu_6(O)_2(O_2CMe)(chp)_3]$; 794, $[Cu_5(O)_2(O_2CMe)(chp)_3]$; 731, $[Cu_4(O)_2(O_2CMe)(chp)_3]$; 662, $[Cu_4(O)_2(O_2CMe)_2(chp)_2]$; 591, $[Cu_4(O)_2(O_2CMe)_3(chp)]$; 522, $[Cu_4(O)_2(O_2CMe)_4]$; 461, $[Cu_4(O)_2(O_2CMe)_3]$; 443, $[Cu_4(O)(O_2CMe)_3]$; 384, $[Cu_3(O)(O_2CMe)_3]$.

$[Cu_8(O)_2(O_2CMe)_3(O_2CH)(chp)_8]$ **4b**. Compound **1** (0.06 g, 0.1 mmol) was allowed to stand in acetone (10 cm^3) for 6 w, during which time a small number of dark green crystals formed which proved suitable for X-ray analysis. The yield (< 5%) prevented any characterisation beyond a crystal structural determination.

$[Cu_8(O)_2(O_2CMe)_4(mhp)_8]$ **5**. *Route* (*a*). Compound **2** (0.352 g, 0.2 mmol) was dissolved in CH_2Cl_2 (15 cm^3) and filtered onto an excess of $[Cu_2(O_2CMe)_4(H_2O)_2]$ (1 g, 2.5 mmol) and allowed to stand for 36 h. The solution was filtered. Diethyl ether diffusion produced a large number of deep blue and a few dark green crystals over a period of 48 h. The deep blue crystals (major product) were shown by elemental analysis and IR spectroscopy to be $[Cu_2(O_2CMe)_4(Hmhp)_2]$, a dimeric copper carboxylate complex similar to $[Cu_2(O_2CMe)_4(Hhp)_2]$ (Hhp = pyridone).[31] Subsequent X-ray diffraction studies showed the dark green crystals to be $[Cu_8(O)_2(O_2CMe)_4(mhp)_8]$ **5**.

Route (*b*). In a similar reaction to that described for **4**, an intimate mixture of $[Cu_2(O_2CMe)_4(H_2O)_2]$ (2.00 g, 5 mmol) and Hmhp (1.2 g, 11 mmol) was heated at 150 °C for 30 min, giving a deep green solid. Removal of acetic acid by distillation under reduced pressure, and unreacted Hmhp by sublimation, followed by extraction with CH_2Cl_2 (30 cm^3) and diethyl ether diffusion gave crystals of both $[Cu_2(O_2CMe)_4(Hmhp)_2]$ and **5**.

For both routes the presence of $[Cu_2(O_2CMe)_4(Hmhp)_2]$ in the final product led to poor analytical data for **5**. No significant peaks were observed by FAB mass spectroscopy (MS) and due to the low purity of the compound no further studies were carried out.

$[Cu_8(O)_2(O_2CMe)_4(bhp)_8]$ **6**. This compound was synthesised by both routes given for **4** starting from **3** or Hbhp respectively. The NMR data are given in Table 10. FAB mass spectrum: *m*/*z* 2095, $[Cu_7(O)_2(O_2CMe)_4(bhp)_8]$; 2017, $[Cu_7(O)_2(O_2CMe)_4(bhp)_7(hp)]$ [hp = loss of Br from bhp]; 1988, $[Cu_8(O)_2(O_2CMe)_4(bhp)_7]$; 1908, $[Cu_8(O)_2(O_2CMe)_4(bhp)_6(hp)]$; 1801, $[Cu_6(O)_2(O_2CMe)_3(bhp)_7]$; 1738, $[Cu_5(O)_2(O_2CMe)_3(bhp)_7]$; 1692, $[Cu_7(O)_2(O_2CMe)_3(bhp)_6]$; 1618, $[Cu_8(O)_2(O_2CMe)_2(bhp)_5(hp)]$; 1551, $[Cu_7(O)_2(O_2CMe)_2(bhp)_5(hp)]$; 1442, $[Cu_8(O)_2(O_2CMe)_2(bhp)_4(hp)]$; 1396, $[Cu_6(O)_2(O_2CMe)_2(bhp)_5]$; 1339, $[Cu_6(O)_2(O_2CMe)(bhp)_5]$; 1272, $[Cu_5(O)_2(O_2CMe)_2(bhp)_5]$; 1165, $[Cu_6(O)_2(O_2CMe)_4(bhp)_3]$; 1102, $[Cu_5(O)_2(O_2CMe)_4(bhp)_3]$; 1050, $[Cu_5(O)_2(O_2CMe)_3(bhp)_3]$; 991, $[Cu_6(O)_2(O_2CMe)_4(bhp)_2]$; 928, $[Cu_5(O)_2(O_2CMe)_4(bhp)_2]$; 867, $[Cu_4(O)_2(O_2CMe)_4(bhp)_2]$; 752, $[Cu_5(O)_2(O_2CMe)(bhp)_2]$; 725, $[Cu_4(O)_2(O_2CMe)_3(bhp)(hp)]$; 612, $[Cu_4(O)_2(O_2CMe)_4(hp)]$; 474, $[Cu_6(O)_2(O_2CMe)]$ or $[Cu_2(bhp)_4]$; 411, $[Cu_5(O)_2(O_2CMe)]$; 329, $[Cu_4(O)(O_2CMe)]$.

$[Cu_8(O)_2(O_2CPh)_4(chp)_8]$ **7** was synthesised by route (*a*) given for **4** but using copper benzoate in place of copper acetate. No significant peaks were observed by FAB MS.

$[Cu_8(O)_2(O_2CPh)_4(bhp)_8]$ **8**. Compound **8** was synthesised by route (*a*) given for **4** but starting from **3** and using copper benzoate in place of copper acetate. FAB mass spectrum: *m*/*z* 2284, $[Cu_8(O)_2(O_2CPh)_3(bhp)_8]$; 2235, $[Cu_8(O)_2(O_2CPh)_4(bhp)_7]$; 2173, $[Cu_7(O)_2(O_2CPh)_4(bhp)_7]$; 2114, $[Cu_8(O)_2(O_2CPh)_3(bhp)_7]$; 1930, $[Cu_7(O)_2(O_2CPh)_2(bhp)_7]$; 1879, $[Cu_7(O)_2(O_2CPh)_3(bhp)_6]$; 1756, $[Cu_7(O)_2(O_2CPh)_2(bhp)_6]$; 1572, $[Cu_6(O)_2(O_2CPh)(bhp)_6]$; 1519, $[Cu_6(O)_2(O_2CPh)_2(bhp)_5]$; 1400, $[Cu_6(O)_2(O_2CPh)(bhp)_5]$; 1277, $[Cu_6(O)_2(bhp)_5]$; 1226, $[Cu_6(O)_2(O_2CPh)(bhp)_4]$; 1052, $[Cu_6(O)_2(O_2CPh)(bhp)_3]$; 989, $[Cu_5(O)_2(O_2CPh)(bhp)_3]$.

$[Cu_8(O)_2(O_2CCF_3)_4(chp)_8]$ **9** was synthesised by route (*a*) given for **4** but using copper trifluoroacetate in place of copper acetate. No significant peaks were observed by FAB MS.

The NMR data for **7**, **8** and **9** are given in Table 10.

$[Cu_2L_4]$. Route (*b*) described above leads to octanuclear complexes if heating is carried out for a short period of time. Extended heating times, with addition of further HL (HL = Hmhp, Hchp or Hbhp) during thermolysis, led to the formation of species which analyse as $[Cu_2L_4]$. For chp and bhp the red compounds formed gave infrared spectra identical with those of authentic samples prepared by other routes,[26,28] however, the dark green dimeric complex $[Cu_2(mhp)_4]$ **10** has not been previously obtained. Analytical data for this compound are included in Table 1, but unfortunately crystals suitable for X-ray analysis were not obtained.

Crystallography.—Crystal data, details of data collection and refined parameters for compounds **4**, **4b**, **5** and **6** are given in Table 2. Atomic coordinates are given in Tables 3 to 6. Selected bond lengths and angles are given in Tables 7 and 8. Unit-cell parameters were also collected for complexes **7** and **8** at 150 K: **7**, monoclinic, $a = 16.53(7)$, $b = 28.38(12)$, $c = 18.67(9)$ Å, $\beta = 90.5(2)°$, $U = 8758$ Å^3; **8**, triclinic, $a = 13.74(5)$, $b = 15.04(6)$, $c = 22.73(11)$ Å, $\alpha = 93.46(8)$, $\beta = 100.31(9)$, $\gamma = 99.05(8)°$, $U = 4544$ Å^3.

Data collection and processing. Data were collected for **4**, **4b** and **6** on a Stoë Stadi-4 four-circle diffractometer equipped with an Oxford Cryosystems low-temperature device[34] with graphite-monochromated Mo-Kα radiation, ω–2θ scans using the learnt-profile method.[35] Data for **5** were collected on an Enraf-Nonius CAD-4 diffractometer using Cu-Kα radiation

Table 2 Experimental data for the X-ray diffraction studies of compounds **4**, **4b**, **5** and **6**

Compound	**4**	**4b**	**5**	**6**
Formula	$C_{48}H_{36}Cl_8Cu_8N_8O_{18}\cdot 4CH_2Cl_2$	$C_{47}H_{34}Cl_8Cu_8N_8O_{18}\cdot 4C_3H_6O$	$C_{56}H_{60}Cu_8N_8O_{18}\cdot 2.5C_6H_6NO\cdot 2H_2O$	$C_{48}H_{36}Br_8Cu_8N_8O_{18}\cdot 1.5CH_2Cl_2$
M	2144	2023	1949	2295
Crystal system	Triclinic	Monoclinic	Monoclinic	Monoclinic
Space group	$P\bar{1}$	$P2_1/n$	$P2_1/n$	$C2/c$
a/Å	13.402(7)	19.463(4)	11.179(3)	20.994(9)
b/Å	15.089(9)	18.949(4)	51.262(8)	17.238(7)
c/Å	18.993(13)	20.530(8)	15.455(2)	27.427(17)
α/°	83.91(4)	90	90	90
β/°	80.35(5)	97.54(2)	98.22(2)	105.96(4)
γ/°	85.74(4)	90	90	90
U/Å^3	3759	7509	8766	9543
Measurement of unit cell				
No. of reflections	22	31	25	44
2θ/°	$28 \leqslant 2\theta \leqslant 32$	$20 \leqslant 2\theta \leqslant 21$	$25 \leqslant 2\theta \leqslant 45$	$24 \leqslant 2\theta \leqslant 26$
Z	2	4	4	4^a
T/K	150.0(1)	150.0(1)	293	293
D_c/g cm^{-3}	1.89	1.79	1.48	1.60
F(000)	2120	3695	3956	4396
Crystal size/mm	0.40 × 0.38 × 0.20	0.36 × 0.34 × 0.24	0.40 × 0.40 × 0.10	0.42 × 0.38 × 0.2
Crystal shape and colour	Dark green tablet	Dark green plate	Dark green tablet	Green plate
Mounting	Oil drop on glass fibre	Oil drop on glass fibre	In capillary with mother-liquor	In capillary with mother-liquor
Radiation	Mo-Kα	Mo-Kα	Cu-Kα	Mo-Kα
μ/mm^{-1}	2.87	2.59	2.86	5.21
Unique data	9770	8264	5304	6254
Observed data [$I > 2\sigma(I)$]	7407	5650	2988	2268
Max. Δ/σ ratio	+0.017	−0.059	+0.013	−0.015
R, R'^{b}	0.0993, 0.1389	0.0638, 0.0708		0.0817, 0.1041
$R1, wR2^{c}$			0.0929, 0.2544	
Weighting scheme, w^{-1}	$w^{-1} = \sigma^2(F) + 0.001F^2$	$w^{-1} = \sigma^2(F) + 0.0005F^2$	$w^{-1} = \sigma^2(F_o^2) + (0.1734P)^{2\,d}$	$w^{-1} = \sigma^2(F) + 0.001\,75F^2$
Goodness of fit	0.884	1.177	1.035	1.267
Largest residuals/e Å^{-3}	+2.57, −1.61	+1.07, −0.84	+1.278, −0.508	+0.99, −0.68

[a] The molecule lies on a two-fold axis. [b] SHELX 76.[32] [c] SHELXL 93.[33] [d] $P = \frac{1}{3}(2F_c^2 + F_o^2)$.

and ω–2θ scans. All data were corrected for Lorentz and polarisation factors. Semi-empirical absorption corrections[36] based on azimuthal measurements were applied to data for all compounds.

Structure analysis and refinement. Structures **4**, **4b** and **6** were solved by direct methods using SHELXS 86.[37] These structures were refined on F using SHELX 76,[32] with Cu, Cl and O atoms anisotropic in **4**; Cu, Cl, O, N and ring C-atoms anisotropic in **4b**; and all non-H atoms and non-C atoms anisotropic in **6**. In all structures H atoms were included at idealised positions [C–H 0.96 Å], and with fixed isotropic thermal parameters [U = 0.05 Å^2 for **4** and **4b**; U = 0.08 Å^2 for **6**]. For **5** the positions of all eight Cu atoms and the two oxo bridges were found by the heavy-atom method using the program PATTY within the DIRDIF suite of programs.[38] The remaining non-hydrogen atoms were located from subsequent ΔF maps while retaining fixed atomic coordinates for the eight Cu atoms. The structure was refined on F^2 using SHELXL 93,[33] with only Cu atoms anisotropic, with the pyridonate rings constrained to be hexagonal, and the acetate ligands restrained to be planar and with each methyl C–O distance tied to a common value. The hydrogen atoms were included in the refinement at idealised positions [C–H 0.96 Å], and with isotropic thermal parameters tied to that of their parent C atom [U(H) = 1.2 U(C) Å^2 for ring carbons; U(H) = 1.5 U(C) Å^2 for methyl groups].

Additional material available from the Cambridge Crystallographic Data Centre comprises atom coordinates, thermal parameters and remaining bond lengths and angles.

Magnetic Measurements.—Variable-temperature magnetic measurements in the region 5–300 K were made on a Faraday balance (Oxford Instruments) and a SQUID magnetometer (Quantum Design). Samples run on the Faraday Balance were placed in a Teflon bucket whereas SQUID samples were sealed in gelatin capsules. In all cases diamagnetic corrections for the sample holders were applied to the data. Diamagnetic corrections for the samples were determined from Pascal's constants[39] for Cu^{2+} and O^{2-}, literature values for $MeCO_2H$,[40] and experimentally determined molar magnetic susceptibilities of 8.448 × 10^{-3} and 15.187 × 10^{-3} emu mol^{-1} for Hchp and Hbhp respectively, measured by the Gouy method at 298 K. The observed and calculated data were refined using in-house software.[41]

Results and Discussion

Synthesis.—We have explored two reactions involving copper with mixed carboxylate–pyridonate ligands. In every case the reactions lead to compounds of formula $[Cu_8(O)_2(O_2CR)_4L_8]$ (where R = Me, Ph or CF_3; L = chp, bhp or mhp).

The first route involves reaction of pre-formed copper pyridonate complexes, either dimeric $[Cu_2(chp)_4]$ **1** or $[Cu_2(bhp)_4]$ **3**, or the hexanuclear copper complex $[Cu_6Na(mhp)_{12}][NO_3]$ **2**, with copper carboxylates in CH_2Cl_2 at room temperature. In all cases the colour of the solution, which is initially a characteristic red for **1** and **3**, becomes dark green and dark green blocks can be grown by ether diffusion. The yields are good for the reaction of **1** or **3** with copper acetate or benzoate, but very poor for reactions involving **2**. The reaction of **2** with copper acetate gives $[Cu_8(O)_2(O_2CMe)_4(mhp)_8]$ **5**, but only as a minor component, while the major product is $[Cu_2(O_2CMe)_4(Hmhp)_2]$.

The second route involves reacting the copper carboxylates with the molten ligand at elevated temperatures (130–150 °C). This route is similar to that developed by Clegg *et al.* to synthesise the dodecanuclear complex $[Co_{12}(OH)_6(O_2CMe)_6$-

Table 3 Atomic coordinates for **4** with estimated standard deviations (e.s.d.s) in parentheses

Atom	*x*	*y*	*z*	Atom	*x*	*y*	*z*
Cu(1)	0.593 65(13)	0.229 27(12)	0.690 42(10)	O(6R)	0.463 5(7)	0.182 0(7)	0.631 8(5)
Cu(2)	0.422 70(13)	0.287 57(12)	0.798 15(10)	C(62R)	0.462 7(11)	0.148 2(10)	0.571 4(8)
Cu(3)	0.616 51(12)	0.213 56(12)	0.851 12(10)	C(63R)	0.539 1(11)	0.162 6(10)	0.511 1(8)
Cu(4)	0.560 48(13)	0.426 34(11)	0.709 91(9)	C(64R)	0.526 9(12)	0.128 3(11)	0.448 9(9)
Cu(5)	0.389 76(13)	0.298 88(12)	0.646 75(9)	C(65R)	0.442 2(12)	0.083 0(10)	0.443 7(9)
Cu(6)	0.462 40(13)	0.086 44(12)	0.775 56(10)	C(66R)	0.373 5(12)	0.067 6(10)	0.506 3(9)
Cu(7)	0.718 42(13)	0.416 19(12)	0.839 02(10)	Cl(6R)	0.264 0(3)	0.013 0(3)	0.509 47(23)
Cu(8)	0.290 56(13)	0.086 11(12)	0.662 45(10)	N(7R)	0.722 7(9)	0.198 8(8)	0.914 3(6)
O(1)	0.526 6(7)	0.190 0(6)	0.787 9(5)	O(7R)	0.704 9(8)	0.346 5(7)	0.930 6(5)
O(2)	0.489 8(7)	0.327 5(6)	0.700 5(5)	C(72R)	0.748 8(10)	0.270 9(9)	0.946 3(8)
N(1R)	0.831 1(9)	0.335 8(8)	0.796 6(7)	C(73R)	0.818 3(12)	0.254 4(11)	0.997 1(9)
O(1R)	0.705 6(7)	0.266 2(7)	0.766 2(5)	C(74R)	0.854 7(13)	0.171 6(11)	1.013 8(10)
C(12R)	0.800 3(10)	0.275 0(9)	0.761 5(8)	C(75R)	0.827 2(13)	0.098 8(12)	0.981 9(9)
C(13R)	0.874 6(12)	0.220 3(11)	0.719 0(9)	C(76R)	0.764 5(11)	0.115 5(10)	0.930 9(8)
C(14R)	0.974 8(13)	0.235 3(11)	0.715 0(9)	Cl(7R)	0.730 6(4)	0.033 6(3)	0.885 8(3)
C(15R)	1.003 7(13)	0.298 0(11)	0.755 4(9)	N(8R)	0.205 9(9)	0.083 3(8)	0.760 0(6)
C(16R)	0.931 2(11)	0.345 7(10)	0.794 4(8)	O(8R)	0.333 6(7)	0.158 9(7)	0.780 1(6)
Cl(1R)	0.954 7(3)	0.429 6(3)	0.845 4(3)	C(82R)	0.243 5(10)	0.131 5(9)	0.802 0(8)
N(2R)	0.596 6(8)	0.552 5(7)	0.716 6(6)	C(83R)	0.187 1(12)	0.145 8(11)	0.870 0(9)
O(2R)	0.744 9(8)	0.492 9(7)	0.751 4(5)	C(84R)	0.093 0(14)	0.112 8(12)	0.888 8(10)
C(22R)	0.687 0(12)	0.564 7(11)	0.734 6(9)	C(85R)	0.056 2(13)	0.063 5(11)	0.844 9(9)
C(23R)	0.718 8(15)	0.652 1(13)	0.735 8(11)	C(86R)	0.114 4(13)	0.050 1(11)	0.778 9(9)
C(24R)	0.656 3(15)	0.721 5(14)	0.722 4(11)	Cl(8R)	0.073 8(3)	−0.008 8(3)	0.716 7(3)
C(25R)	0.560 7(15)	0.711 8(13)	0.704 2(11)	C(11A)	0.275 6(11)	0.419 6(10)	0.738 8(9)
C(26R)	0.538 9(13)	0.624 1(11)	0.700 1(9)	C(21A)	0.204 1(13)	0.497 7(11)	0.752 3(9)
Cl(2R)	0.421 9(3)	0.601 5(3)	0.680 3(3)	O(11A)	0.304 6(7)	0.376 3(7)	0.794 8(6)
N(3R)	0.598 0(9)	0.490 9(8)	0.877 3(7)	O(21A)	0.298 9(8)	0.398 2(7)	0.678 0(6)
O(3R)	0.524 1(8)	0.402 5(6)	0.814 4(5)	C(12A)	0.673 9(12)	0.367 8(10)	0.578 6(9)
C(32R)	0.511 2(10)	0.465 7(9)	0.857 4(8)	C(22A)	0.726 3(13)	0.389 7(12)	0.500 9(10)
C(33R)	0.418 1(11)	0.505 5(9)	0.885 2(8)	O(12A)	0.639 6(8)	0.430 6(7)	0.615 0(5)
C(34R)	0.412 6(12)	0.573 0(1)	0.928 8(8)	O(22A)	0.668 9(7)	0.284 3(7)	0.599 9(5)
C(35R)	0.500 6(12)	0.601 3(10)	0.945 0(9)	C(13A)	0.421 3(11)	0.218 0(10)	0.945 8(8)
C(36R)	0.590 3(12)	0.558 2(10)	0.916 5(9)	C(23A)	0.365 1(13)	0.187 3(11)	1.018 9(9)
Cl(3R)	0.707 5(3)	0.588 4(3)	0.933 4(3)	O(13A)	0.517 8(8)	0.198 4(7)	0.939 0(6)
N(4R)	0.310 3(9)	0.292 1(8)	0.569 8(7)	O(23A)	0.374 5(7)	0.259 9(7)	0.902 5(6)
O(4R)	0.207 1(8)	0.190 9(7)	0.635 2(6)	C(14A)	0.670 4(11)	0.044 0(10)	0.704 9(8)
C(42R)	0.226 1(12)	0.242 2(10)	0.576 4(9)	C(24A)	0.757 5(14)	−0.024 9(12)	0.696 6(10)
C(43R)	0.171 8(14)	0.250 0(12)	0.520 7(10)	O(14A)	0.587 8(8)	0.017 1(7)	0.744 1(6)
C(44R)	0.196 0(13)	0.303 1(11)	0.460 1(10)	O(24A)	0.681 0(7)	0.121 1(7)	0.674 6(5)
C(45R)	0.279 2(13)	0.359 0(12)	0.455 3(10)	C(1S)	0.156 2(17)	0.376 9(14)	−0.060 4(12)
C(46R)	0.332 0(11)	0.346 6(10)	0.509 1(8)	Cl(11)	0.129 6(4)	0.493 7(4)	−0.053 2(3)
Cl(4R)	0.441 2(3)	0.403 8(3)	0.504 85(25)	Cl(21)	0.088 0(4)	0.312 5(5)	0.009 6(3)
N(5R)	0.396 5(9)	−0.029 6(8)	0.797 6(7)	C(2S)	0.873 9(23)	0.176 8(20)	0.523 0(16)
O(5R)	0.357 6(8)	−0.028 4(7)	0.684 7(5)	Cl(12)	0.951 4(5)	0.090 8(4)	0.551 2(5)
C(52R)	0.361 2(12)	−0.069 8(11)	0.747 3(9)	Cl(22)	0.874 7(9)	0.185 8(6)	0.428 7(5)
C(53R)	0.336 1(12)	−0.159 4(11)	0.763 0(9)	C(3S)	−0.071 1(23)	0.482 7(19)	0.611 9(17)
C(54R)	0.344 1(13)	−0.202 5(12)	0.825 4(10)	Cl(13)	−0.004 7(7)	0.573 7(7)	0.636 7(5)
C(55R)	0.383 6(13)	−0.161 1(11)	0.879 7(10)	Cl(23)	0.009 1(7)	0.408 4(5)	0.572 2(4)
C(56R)	0.405 1(12)	−0.074 9(11)	0.860 9(9)	C(4S)	0.014(3)	0.303(3)	0.203(3)
Cl(5R)	0.444 3(3)	−0.012 2(3)	0.921 45(22)	Cl(14)	−0.100 1(7)	0.272 1(7)	0.181 3(6)
N(6R)	0.383 0(9)	0.098 5(8)	0.567 9(7)	Cl(24)	0.098 0(11)	0.204 5(10)	0.199 6(12)

(mhp)$_{12}$].[42] The advantages of this synthesis are that the carboxylic acid produced during the reaction can be removed by distillation under reduced pressure, and unreacted pyridone can be retrieved by sublimation from the reaction mixture, again at reduced pressure. When Hchp or Hbhp are used a red paste results whereas reaction in molten Hmhp leads to a green paste. Extraction of these pastes with CH_2Cl_2 gave solutions from which the relevant octanuclear compounds could be obtained in high yields by ether diffusion. Curiously for Hchp and Hbhp the CH_2Cl_2 solutions were initially red, but rapidly became dark green.

The existence of two complementary routes to the same materials led us to investigate this second reaction more closely. In particular it seemed apparent, from the red colour observed on heating the copper carboxylates in molten Hchp or Hbhp, that reaction was leading to initial formation of [Cu_2L_4], which on dissolution in CH_2Cl_2 was reacting further with residual copper carboxylate to give the octanuclear [$Cu_8(O)_2(O_2CR)_4L_8$] compounds. In order to demonstrate this the reaction of [$Cu_2(O_2CMe)_4(H_2O)_2$] with a four-fold equivalent of Hchp was studied using thermal methods.

Differential scanning calorimetry studies indicate that the reaction begins at *ca.* 75 °C, and TGA indicates that this endothermic step is associated with a loss of 1.5% of sample weight. Both observations are consistent with loss of one co-ordinated water molecule from copper acetate. A much larger endotherm, commencing at 115 °C with a peak maximum at 120 °C, can be attributed to loss of the second water (2.5% of sample weight by TGA). At 128 °C a third endotherm is observed which we can assign to melting of Hchp, its reaction with copper acetate and loss of acetic acid. Thermogravimetric analysis showed a gradual weight loss over the temperature range 128–150 °C, beyond which no further reaction was observed either by DSC or TGA up 230 °C. The total observed weight loss up to 150 °C was 37 ± 1%, which is somewhat

Table 4 Atomic coordinates for **4b** with e.s.d.s in parentheses

Atom	*x*	*y*	*z*
Cu(1)	0.908 56(9)	0.588 45(9)	0.239 81(9)
Cu(2)	0.806 74(9)	0.703 36(9)	0.226 95(9)
Cu(3)	0.939 42(9)	0.726 01(9)	0.318 19(9)
Cu(4)	0.787 23(9)	0.579 88(9)	0.318 07(9)
Cu(5)	0.774 63(9)	0.575 26(9)	0.143 81(8)
Cu(6)	0.926 64(9)	0.711 11(9)	0.147 86(9)
Cu(7)	0.869 79(9)	0.669 64(9)	0.454 34(9)
Cu(8)	0.841 47(9)	0.642 49(9)	0.008 20(9)
O(1)	0.906 5(4)	0.691 6(4)	0.232 7(4)
O(2)	0.806 4(4)	0.599 9(4)	0.231 9(4)
Cl(1R)	0.976 28(22)	0.630 04(23)	0.587 25(20)
N(1R)	0.961 3(6)	0.623 3(6)	0.460 0(6)
O(1R)	0.937 2(5)	0.627 6(5)	0.349 9(5)
C(12R)	0.979 2(8)	0.606 0(7)	0.401 5(7)
C(13R)	1.037 8(7)	0.565 1(7)	0.396 0(8)
C(14R)	1.078 6(8)	0.545 5(7)	0.452 2(8)
C(15R)	1.062 1(7)	0.564 4(7)	0.513 8(7)
C(16R)	1.004 1(8)	0.602 7(7)	0.513 7(7)
Cl(2R)	0.631 79(24)	0.540 7(3)	0.299 49(22)
N(2R)	0.733 2(6)	0.557 4(6)	0.392 1(6)
O(2R)	0.830 4(5)	0.577 5(5)	0.467 0(5)
C(22R)	0.766 8(8)	0.559 4(7)	0.457 3(7)
C(23R)	0.728 8(8)	0.539 8(7)	0.508 0(7)
C(24R)	0.662 5(9)	0.517 1(8)	0.494 1(9)
C(25R)	0.629 1(9)	0.517 0(8)	0.429 3(9)
C(26R)	0.669 3(9)	0.538 9(8)	0.382 4(8)
Cl(3R)	0.781 60(23)	0.743 51(23)	0.564 08(20)
N(3R)	0.777 0(6)	0.714 6(6)	0.440 0(6)
O(3R)	0.788 2(5)	0.680 6(5)	0.336 9(5)
C(32R)	0.749 8(7)	0.713 0(7)	0.375 8(7)
C(33R)	0.685 9(7)	0.743 2(7)	0.355 7(7)
C(34R)	0.649 1(8)	0.775 6(8)	0.400 6(8)
C(35R)	0.677 5(8)	0.775 5(8)	0.466 7(8)
C(36R)	0.740 9(8)	0.744 9(8)	0.484 4(7)
Cl(4R)	0.739 08(23)	0.421 26(22)	0.152 14(21)
N(4R)	0.738 0(5)	0.519 5(6)	0.064 1(6)
O(4R)	0.747 2(5)	0.611 4(5)	−0.005 4(5)
C(42R)	0.727 2(7)	0.547 2(8)	0.003 5(7)
C(43R)	0.692 2(8)	0.507 0(8)	−0.048 2(7)
C(44R)	0.671 1(8)	0.439 3(9)	−0.036 8(9)
C(45R)	0.683 3(8)	0.412 0(8)	0.026 6(9)
C(46R)	0.717 9(8)	0.451 1(8)	0.073 2(7)
Cl(5R)	0.980 5(3)	0.865 20(24)	0.160 52(23)
N(5R)	0.958 7(6)	0.767 1(6)	0.073 0(6)
O(5R)	0.934 0(5)	0.673 2(5)	0.003 3(5)
C(52R)	0.959 1(7)	0.736 0(8)	0.012 2(8)
C(53R)	0.988 1(8)	0.773 8(9)	−0.035 7(8)
C(54R)	1.016 0(9)	0.836 8(9)	−0.023 5(9)
C(55R)	1.016 9(9)	0.867 9(8)	0.038 9(9)
C(56R)	0.984 5(7)	0.829 2(9)	0.082 5(7)
Cl(6R)	0.873 78(20)	0.532 57(20)	−0.106 34(17)
N(6R)	0.878 7(5)	0.545 1(5)	0.020 1(5)
O(6R)	0.872 2(4)	0.568 7(4)	0.126 7(4)
C(62R)	0.893 9(6)	0.525 8(6)	0.084 2(7)
C(63R)	0.928 9(7)	0.462 7(7)	0.100 5(6)
C(64R)	0.949 6(6)	0.422 2(7)	0.051 8(7)
C(65R)	0.932 3(7)	0.439 6(6)	−0.014 1(7)
C(66R)	0.897 1(7)	0.501 8(7)	−0.026 6(6)
Cl(7R)	1.094 36(21)	0.750 62(24)	0.320 61(21)
N(7R)	0.999 2(5)	0.761 5(5)	0.397 7(5)
O(7R)	0.907 3(5)	0.763 9(4)	0.456 3(4)
C(72R)	0.970 8(8)	0.778 6(7)	0.452 2(7)
C(73R)	1.014 4(9)	0.814 3(7)	0.503 4(7)
C(74R)	1.081 7(8)	0.828 5(7)	0.498 1(7)
C(75R)	1.111 3(8)	0.807 8(7)	0.441 9(7)
C(76R)	1.066 7(7)	0.776 2(7)	0.394 5(6)
Cl(8R)	0.788 81(21)	0.750 72(20)	−0.118 41(18)
N(8R)	0.805 9(5)	0.7405(5)	0.009 5(5)
O(8R)	0.830 4(4)	0.720 7(4)	0.117 3(4)
C(82R)	0.802 6(7)	0.761 5(7)	0.070 7(7)
C(83R)	0.766 2(7)	0.825 0(7)	0.083 3(7)
C(84R)	0.737 5(7)	0.863 0(8)	0.030 4(7)
C(85R)	0.744 1(7)	0.842 9(7)	−0.032 6(8)
C(86R)	0.777 5(7)	0.782 0(7)	−0.040 6(6)
C(11A)	0.666 2(7)	0.668 2(8)	0.173 3(7)
C(21A)	0.593 5(10)	0.687 1(11)	0.173 8(11)
O(11A)	0.706 8(4)	0.711 0(5)	0.202 4(4)
O(21A)	0.681 9(4)	0.610 4(5)	0.147 7(4)
O(23A)	0.809 5(4)	0.806 7(4)	0.237 7(4)
C(12A)	0.862 1(7)	0.455 3(7)	0.290 5(9)
O(12A)	0.814 1(5)	0.481 9(4)	0.317 2(4)
O(22A)	0.906 8(4)	0.487 4(4)	0.260 3(4)
C(13A)	0.859 3(8)	0.843 3(7)	0.260 8(7)
O(13A)	0.916 2(5)	0.823 4(4)	0.295 4(5)
C(14A)	1.042 5(7)	0.620 0(8)	0.202 1(7)
C(24A)	1.121 7(10)	0.613 2(13)	0.215 6(12)
O(14A)	1.021 6(5)	0.671 9(5)	0.164 2(5)
O(24A)	1.008 5(4)	0.579 9(4)	0.231 0(5)
O(1S)	0.029 2(7)	0.069 7(8)	0.344 7(7)
C(11S)	0.040 1(9)	−0.046 9(10)	0.313 0(9)
C(21S)	0.011 8(9)	0.007 7(10)	0.350 7(9)
C(31S)	−0.037 7(10)	−0.011 7(10)	0.399 1(9)
O(2S)	0.005 1(10)	0.293 3(10)	0.192 3(10)
C(12S)	0.043 4(14)	0.310 4(14)	0.237 9(14)
C(22S)	0.066 3(11)	0.390 8(12)	0.251 1(11)
C(32S)	0.069 3(12)	0.250 4(13)	0.285 3(12)
O(3S)	0.180 3(12)	0.023 8(14)	0.159 3(12)
C(13S)	0.154 0(18)	0.071 0(19)	0.188 1(18)
C(23S)	0.080 9(17)	0.087 9(16)	0.166 3(16)
C(33S)	0.192 6(15)	0.086 5(15)	0.252 1(15)
O(4S)	0.236 7(8)	0.273 5(9)	0.271 9(8)
C(14S)	0.276 9(13)	0.327 5(15)	0.278 5(13)
C(24S)	0.340 4(14)	0.320 7(15)	0.331 5(14)
C(34S)	0.270 7(14)	0.388 8(15)	0.235 5(14)

greater than that calculated for loss of two water and four acetic acid molecules from the substrate (ideal 30%). This disparity is accounted for by the partial volatilisation of Hchp.

These observations suggest that the reaction in the molten ligand occurs in three stages, as shown in Scheme 1. On dissolution of $[Cu_2(chp)_4]$ the octanuclear species is formed by reaction of the newly synthesised dimeric species with unreacted copper carboxylate.

Scheme 1 is consistent with the red colour observed in the syntheses of both **4** and **6** by route (*b*), and also with the isolation of $[Cu_2(O_2CMe)_4(Hmhp)_2]$ as the major product of the reactions intended to produce **5**. It also indicates that routes (*a*) and (*b*) are essentially identical, differing only in that in route (*b*) the dimeric copper pyridonate complexes are prepared *in situ*, rather than isolated beforehand. Exhaustive thermolysis

$$[Cu_2(O_2CMe)_4(H_2O)_2] + 4\,Hchp$$

$$(i)\downarrow$$

$$[Cu_2(O_2CMe)_4(H_2O)(Hchp)] + 3\,Hchp$$

$$(ii)\downarrow$$

$$[Cu_2(O_2CMe)_4(Hchp)_2] + 2\,Hchp$$

$$(iii)\downarrow$$

$$[Cu_2(chp)_4]$$

Scheme 1 (*i*) 75 °C, $-H_2O$; (*ii*) 115 °C, $-H_2O$; (*iii*) 128–150 °C, $-4\,MeCO_2H$

Table 5 Atomic coordinates for **5** with e.s.d.s in parentheses

Atom	*x*	*y*	*z*	Atom	*x*	*y*	*z*
Cu(1)	3475(3)	1233(1)	2143(2)	N(7R)	6391(12)	583(2)	2472(8)
Cu(2)	3829(3)	1157(1)	4037(2)	C(72R)	6120(11)	323(3)	2613(8)
Cu(3)	5413(3)	847(1)	2950(2)	C(73R)	6760(14)	126(2)	2265(10)
Cu(4)	1805(3)	861(1)	2926(2)	C(74R)	7671(13)	188(3)	1776(9)
Cu(5)	1953(3)	1553(1)	3246(2)	C(75R)	7942(12)	448(3)	1635(9)
Cu(6)	5487(3)	1535(1)	3234(2)	C(76R)	7303(13)	645(2)	1983(9)
Cu(7)	3586(3)	326(1)	2741(2)	C(77R)	7501(28)	909(5)	1821(18)
Cu(8)	3794(3)	2074(1)	3485(2)	O(7R)	5335(14)	268(3)	3094(10)
O(1)	4814(11)	1192(2)	3094(8)	N(8R)	4491(12)	2004(3)	4691(7)
O(2)	2460(12)	1202(3)	3091(8)	C(82R)	4700(14)	1740(3)	4852(9)
N(1R)	3802(12)	384(3)	1523(7)	C(83R)	5098(15)	1654(2)	5697(11)
C(12R)	3983(13)	646(3)	1349(9)	C(84R)	5288(14)	1832(3)	6381(8)
C(13R)	4099(15)	725(2)	505(11)	C(85R)	5079(14)	2096(3)	6221(8)
C(14R)	4034(15)	543(4)	−165(8)	C(86R)	4680(13)	2182(2)	5376(10)
C(15R)	3853(15)	281(3)	8(9)	C(87R)	4439(23)	2458(5)	5097(15)
C(16R)	3737(14)	201(2)	852(10)	O(8R)	4493(12)	1598(3)	4156(8)
C(17R)	3618(25)	−72(5)	1135(17)	C(23A)	7028(21)	877(5)	5602(14)
O(1R)	4026(12)	792(3)	2010(8)	C(13A)	6118(23)	916(4)	4785(16)
N(2R)	774(12)	568(3)	3173(9)	O(13A)	6398(13)	830(3)	4086(9)
C(22R)	1058(12)	319(3)	2908(9)	O(23A)	5182(13)	1048(3)	4932(9)
C(23R)	467(15)	103(2)	3189(10)	C(21A)	1302(21)	1337(5)	5783(14)
C(24R)	−408(14)	136(3)	3735(11)	C(11A)	1882(22)	1344(5)	4954(16)
C(25R)	−692(12)	385(4)	4000(9)	O(11A)	2813(14)	1203(3)	4979(9)
C(26R)	−101(14)	601(3)	3719(9)	O(21A)	1417(14)	1487(3)	4364(9)
C(27R)	−285(25)	865(5)	4005(17)	C(22A)	178(23)	1091(5)	420(16)
O(2R)	1826(14)	314(3)	2359(10)	C(12A)	1055(23)	1067(5)	1232(16)
N(3R)	3371(12)	299(3)	3970(7)	O(22A)	2062(14)	1195(3)	1187(9)
C(32R)	3136(13)	543(2)	4302(9)	O(12A)	842(13)	934(3)	1821(9)
C(33R)	2933(14)	567(2)	5165(10)	C(24A)	6157(22)	1491(5)	580(15)
C(34R)	2965(14)	348(3)	5695(7)	C(14A)	5479(24)	1453(4)	1384(16)
C(35R)	3199(14)	104(3)	5363(9)	O(24A)	4486(14)	1338(3)	1246(9)
C(36R)	3403(13)	80(2)	4501(10)	O(14A)	6049(14)	1545(3)	2094(9)
C(37R)	3616(26)	−165(5)	4087(17)	N(11S)	6073(13)	2533(2)	2114(8)
O(3R)	3171(12)	739(3)	3773(8)	C(12S)	6068(13)	2477(2)	1233(8)
N(4R)	858(12)	1850(2)	3019(9)	C(13S)	6415(15)	2666(3)	676(7)
C(42R)	1219(11)	2094(3)	3358(8)	C(14S)	6767(16)	2912(3)	998(10)
C(43R)	474(15)	2309(2)	3167(10)	C(15S)	6773(16)	2968(2)	1879(11)
C(44R)	−633(13)	2281(3)	2637(10)	C(16S)	6426(15)	2779(3)	2436(8)
C(45R)	−995(11)	2038(3)	2298(9)	O(11S)	6445(19)	2820(4)	3230(13)
C(46R)	−249(13)	1823(2)	2489(9)	C(17S)	5776(25)	2217(5)	958(14)
C(47R)	−525(25)	1557(5)	2126(17)	O(1W)	4085(62)	2076(13)	8790(43)
O(4R)	2222(14)	2104(3)	3879(9)	N(31S)	7451(33)	1582(7)	8218(24)
N(5R)	6684(11)	1800(3)	3721(8)	C(32S)	8656(38)	1560(7)	8099(24)
C(52R)	6410(10)	2064(3)	3635(8)	C(33S)	9518(29)	1725(9)	8545(30)
C(53R)	7225(14)	2249(2)	4026(10)	C(34S)	9175(44)	1913(8)	9111(27)
C(54R)	8314(12)	2169(3)	4502(9)	C(35S)	7971(51)	1935(7)	9230(23)
C(55R)	8587(10)	1905(3)	4587(9)	C(36S)	7109(33)	1770(9)	8784(27)
C(56R)	7772(13)	1721(2)	4197(9)	O(31S)	5699(47)	1734(13)	8705(32)
C(57R)	7967(24)	1439(5)	4250(16)	C(37S)	8912(62)	1428(15)	7622(51)
O(5R)	415(13)	2124(3)	3147(9)	N(41S)	4478(30)	1325(6)	8142(22)
N(6R)	3092(12)	2104(3)	2265(7)	C(42S)	4960(33)	1141(8)	7630(23)
C(62R)	2840(13)	1861(2)	1879(9)	C(43S)	4336(47)	911(7)	7402(25)
C(63R)	2356(14)	1845(2)	1001(9)	C(44S)	3230(47)	865(6)	7687(29)
C(64R)	2124(13)	2071(3)	508(7)	C(45S)	2749(33)	1049(8)	8199(26)
C(65R)	2376(14)	2313(3)	894(9)	C(46S)	3372(30)	1279(6)	8427(20)
C(66R)	2860(13)	2330(2)	1772(9)	C(47S)	3000(46)	1438(10)	8972(35)
C(67R)	3087(21)	2588(4)	2261(14)	O(41S)	5710(134)	1175(16)	7405(69)
O(6R)	3006(13)	1680(3)	2412(9)	O(2W)	457(33)	242(7)	219(23)

reactions lead to complete reaction of the copper carboxylate substrates, and hence to isolation of exclusively $[Cu_2L_4]$ complexes. Such a dimer has not been crystallographically characterised for the mhp ligand, rather the hexanuclear metallocrown **2** has been found. The analytical and spectroscopic data obtained here are consistent with formation not of **2**, but of $[Cu_2(mhp)_4]$. In the absence of a structure determination such an assignment must remain tentative.

A third route to an octanuclear complex has also been observed. Addition of **1** to acetone leads over a period of six weeks to formation, in very low yield, of dark green crystals which X-ray analysis showed to be $[Cu_8(O)_2(O_2CMe)_3(O_2CH)(chp)_8]$ **4b**. This was an unexpected result, and is probably due to the presence of traces of the carboxylic acids in the acetone used. In related experiments, designed to synthesise mixed-metal complexes from the reaction of **1** with salts of other metals, we have found that the presence of acetate counter ions invariably leads to the formation of **4**.[43] These observations suggest a strong tendency for the formation of these octanuclear complexes in the presence of acetate and pyridonate ligands.

Crystal Structures.—The compounds all form dark green crystals which are unstable outside mother-liquor at room

Table 6 Atomic coordinates for **6** with e.s.d.s in parentheses

Atom	*x*	*y*	*z*
Cu(1)	0.000 00(0)	0.626 5(3)	0.250 00(0)
Cu(2)	0.000 00(0)	0.457 0(3)	0.250 00(0)
Cu(3)	0.013 93(17)	0.538 48(21)	0.155 07(11)
Cu(4)	0.128 26(17)	0.544 94(22)	0.303 02(12)
Cu(7)	0.186 48(18)	0.547 96(23)	0.196 54(12)
O(1)	−0.035 8(9)	0.541 3(10)	0.203 4(6)
Br(1R)	0.272 52(22)	0.667 3(3)	0.136 82(17)
N(1R)	0.162 2(12)	0.654 0(13)	0.169 2(8)
O(1R)	0.071 5(9)	0.620 8(10)	0.195 3(6)
C(11R)	0.195 6(16)	0.705 4(19)	0.147 7(11)
C(12R)	0.175 3(17)	0.774 9(20)	0.141 0(12)
C(13R)	0.118 8(19)	0.801 5(23)	0.149 6(12)
C(14R)	0.081 9(15)	0.750 8(19)	0.170 2(10)
C(15R)	0.104 5(16)	0.674 1(18)	0.177 9(10)
Br(2R)	0.197 54(21)	0.451 5(3)	0.403 16(14)
N(2R)	0.228 6(11)	0.533 2(13)	0.327 1(8)
O(2R)	0.238 8(10)	0.598 0(11)	0.258 3(8)
C(21R)	0.255 4(16)	0.499 0(18)	0.369 5(11)
C(22R)	0.322 8(18)	0.494 0(20)	0.391 0(13)
C(23R)	0.360 9(20)	0.525 2(20)	0.365 7(13)
C(24R)	0.334 5(16)	0.558 1(18)	0.319 2(11)
C(25R)	0.268 7(17)	0.566 7(19)	0.301 5(12)
Br(3R)	0.318 38(21)	0.444 0(3)	0.193 73(18)
N(3R)	0.202 8(12)	0.442 6(13)	0.224 2(9)
O(3R)	0.113 8(9)	0.463 6(12)	0.251 9(6)
C(31R)	0.250 4(20)	0.393 5(24)	0.219 9(13)
C(32R)	0.252 3(19)	0.313 9(22)	0.229 6(12)
C(33R)	0.203 2(17)	0.287 5(21)	0.243 9(12)
C(34R)	0.155 8(17)	0.339 5(20)	0.253 6(12)
C(35R)	0.157 2(17)	0.415 5(19)	0.244 0(10)
Br(4R)	0.074 62(20)	0.623 1(3)	0.441 98(13)
N(4R)	−0.048 1(12)	0.556 0(13)	0.406 6(7)
O(4R)	−0.143 2(11)	0.496 6(14)	0.367 5(7)
C(41R)	−0.008 8(16)	0.587 8(19)	0.446 4(12)
C(42R)	−0.021 0(17)	0.595 6(19)	0.493 0(12)
C(43R)	−0.085 4(17)	0.567 1(19)	0.494 1(13)
C(44R)	−0.127 1(17)	0.535 0(19)	0.452 9(11)
C(45R)	−0.108 8(17)	0.531 3(19)	0.406 1(12)
C(11A)	0.030 7(15)	0.375 8(19)	0.350 1(12)
C(21A)	0.054 6(20)	0.307 6(22)	0.377 4(14)
O(11A)	0.020 5(10)	0.373 7(10)	0.302 8(6)
O(21A)	0.019 5(10)	0.435 5(11)	0.371 9(6)
C(12A)	0.103 2(16)	0.701 4(19)	0.329 1(11)
C(22A)	0.122 7(15)	0.769 0(17)	0.364 1(10)
O(12A)	0.140 5(11)	0.643 1(12)	0.339 8(8)
O(22A)	0.053 3(10)	0.708 7(10)	0.294 5(7)
C(1S)	0.000 00(0)	0.187(5)	0.250 00(0)
Cl(1S)	0.065 5(11)	0.146 9(12)	0.277 9(12)
C(2S)	0.500 00(0)	0.380(4)	0.250 00(0)
Cl(2S)	0.500 4(8)	0.436 6(8)	0.302 8(6)

temperature. Data collection was therefore carried out either on a crystal encapsulated within an oil drop at 150 K,[34] or on crystals mounted in a capillary with mother-liquor. The crystals of complexes **7** and **8** were insufficiently stable to allow data collection, losing crystallinity in a matter of hours even at 150 K, and only unit-cell parameters can be reported. The volume of the unit cells, combined with analytical and spectroscopic data, allows us to be confident that these complexes are very similar to the structurally characterised compounds **4**, **4b**, **5** and **6**.

The structure of **4** is shown in Fig. 1, **5** and **6** are essentially identical to **4**, differing only in the substituent at the 6 position on the pyridonate ring. At the centre of the structure is an edge-sharing oxygen-centred bitetrahedron of copper atoms encapsulated within two $[CuL_4]^{2-}$ groups. Compound **4b** differs from **4** in having a bridging formate group in place of one of the four bridging acetate groups. Selected bond lengths and angles are given in Tables 7 and 8 respectively.

There are two chemically distinct types of copper site in the bitetrahedron. The first type comprises the two copper atoms forming the shared edge [Cu(1) and Cu(2)]. They are six-co-ordinate, bound to the two μ_4-O atoms at the centres of the tetrahedra, two μ_2-oxygen atoms derived from pyridonate ligands and two oxygen atoms from acetate ligands. The two pyridonate oxygens are *trans* to each other, and the Cu–O bonds to these atoms are longer, between 2.29 and 2.44 Å, than the bonds to the remaining four oxygens, which vary from 1.94 to 2.01 Å. Therefore these coppers have a 4 + 2 co-ordination geometry typical for Cu^{II}, although distortion of this geometry is considerably greater than merely tetragonal elongation of an octahedron. The *trans* angles within the equatorial plane are between 168 and 172°, while those between the axial pyridonate oxygens vary from 170 to 177°. The *cis* angles at these edge coppers vary from 75 to 103°, with the largest deviations involving angles between the axial pyridonate oxygens and the oxygens in the equatorial plane. The angles subtended at the coppers by the μ_4-oxygens are also markedly acute, averaging 83.2 ± 0.9°.

The second chemically distinct type of copper site within the central bitetrahedra comprises the four coppers at the external vertices [Cu(3), Cu(4), Cu(5) and Cu(6)]. These are each four-co-ordinate, bound to one μ_4-oxo atom, one μ_2-pyridonate oxygen, one acetate oxygen and one nitrogen atom from a pyridonate ligand. The co-ordination geometry is clearly based on square planar, but distorted with *cis* angles varying from 86 to 96°, and *trans* angles as low as *ca.* 154°. The distortion is therefore best described as a folding of a square plane towards a tetrahedron. The bond lengths display a trend, which, although not statistically significant for every structure, is repeated within each compound. Thus the shortest bonds are those from copper to the μ_4-oxo atoms [1.865(10)–1.917(13) Å]. Next shortest are those to the carboxylate oxygens, ranging from 1.920(14) to 1.976(18) Å. The longest bonds, and again there is some overlap with the previous range, this time for **5** and **6**, are to the atoms from pyridonate ligands.

This edge-sharing oxo-centred bitetrahedron appears to be new in the co-ordination chemistry of copper(II). The closest related species is a complex of 3-(benzylimino)butan-2-one oxime, $[Cu_6(\mu_4\text{-}O)_2L_6(H_2O)][ClO_4]_2$ **11** [where L = $PhCH_2\text{-}N{=}C(Me)C(Me){=}N\text{-}OH$].[13] In **11** the μ_4-oxo atoms have close to a trigonal-pyramidal environment, where they lie within a plane of three copper atoms, thus having three angles close to 120°, with contacts of *ca.* 1.90 Å. There is a much longer contact (*ca.* 2.40 Å) to a fourth copper, this fourth copper coming from the second trigonal plane of coppers within the cation.[13] In the compounds reported here the Cu–μ-O distances are more nearly equivalent, ranging from 1.86 to 1.98 Å, with the longest bonds to the Cu atoms in the shared edge. Four of the angles at the μ_4-O atoms are close to 109°, but that involving the two coppers in the shared edge is somewhat smaller, varying from *ca.* 95 to 98°. The sixth angle, which is that between the two coppers at the external vertices is very obtuse in every case, averaging 136 ± 4°.

The comparative dimensions of the edge-sharing oxo-centred bitetrahedra in **4**, **4b**, **5**, **6** and **11** are given in Table 9. As can be seen the Cu···Cu distances are strongly dependent on the bridging group. For the shared edge bridged by the two μ_4-oxo atoms the distance varies from 2.922(4) to 2.955(2) Å. In **4** and **6** the edges bridged by acetates are significantly shorter than those bridged by μ_2-O atoms from pyridonate groups, whilst in **4b** and **5** this difference is not statistically significant. The unbridged external edges are much longer at between 3.48 and 3.58 Å.

The surrounding $[CuL_4]^{2-}$ show much less distortion in the copper co-ordination sphere than is found within the bitetrahedra. The copper sites are each four-co-ordinate, bound to a *trans* array of two N and two O atoms from pyridonate ligands, with bond angles closer to those expected for square-planar geometry. The Cu–N and Cu–O bond lengths show an interesting dependence on the nature of pyridonate. For the chp

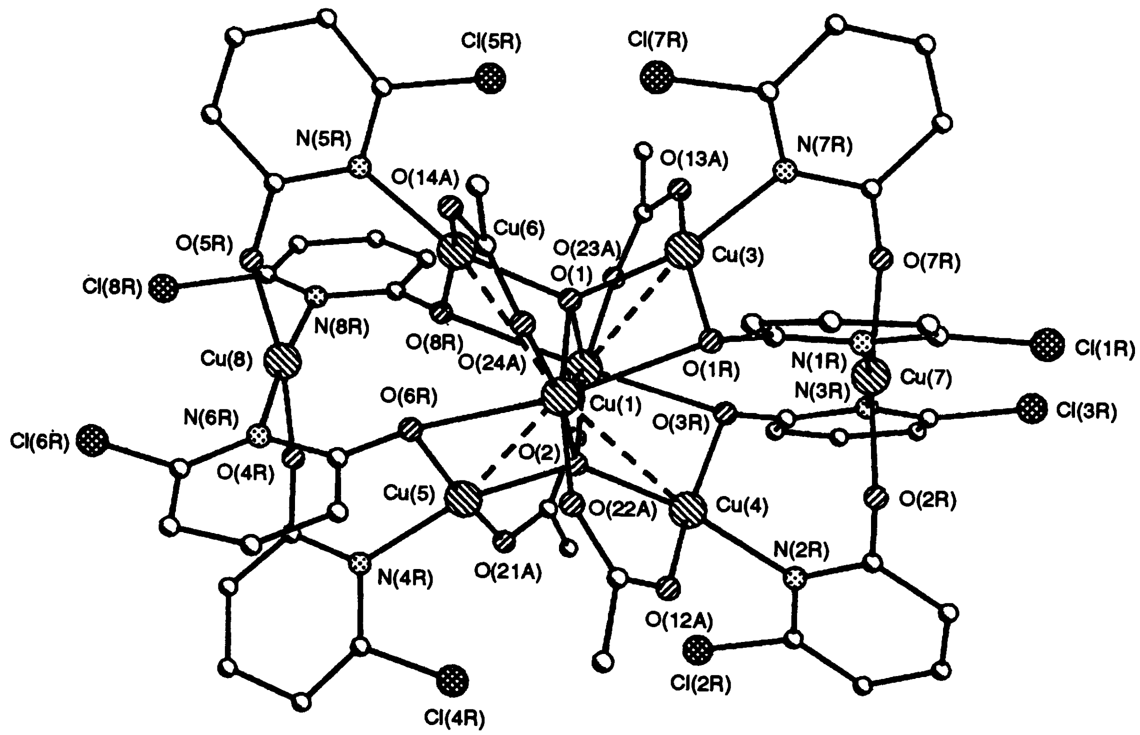

Fig. 1 The structure of **4** in the crystal, showing the atom numbering scheme

Table 7 Selected bond lengths (Å) for compounds **4**, **4b**, **5** and **6**

Compound	**4**	**4b**	**5**	**6**[a]	Compound	**4**	**4b**	**5**	**6**[a]
Bonds involving coppers in shared edge									
Cu(1)–O(1)	1.969(9)	1.961(9)	1.953(13)	1.958(17)	Cu(2)–O(1)	1.952(9)	1.943(9)	1.956(13)	1.945(17)
Cu(1)–O(2)	1.959(10)	1.986(9)	1.983(13)	*b*	Cu(2)–O(2)	1.974(10)	1.963(9)	1.973(13)	*b*
Cu(1)–O(1R)	2.376(10)	2.375(9)	2.359(14)	2.397(18)	Cu(2)–O(3R)	2.356(10)	2.372(10)	2.286(14)	2.378(19)
Cu(1)–O(6R)	2.407(10)	2.367(8)	2.403(14)	*b*	Cu(2)–O(8R)	2.437(10)	2.381(8)	2.377(14)	*b*
Cu(1)–O(22A)	1.975(10)	1.962(8)	2.010(20)	2.000(20)	Cu(2)–O(11A)	2.000(11)	1.950(9)	1.985(14)	2.001(19)
Cu(1)–O(24A)	1.965(10)	1.984(9)	1.990(20)	*b*	Cu(2)–O(23A)	1.989(11)	1.971(9)	1.981(14)	*b*
Bonds involving coppers at external vertices of bitetrahedron									
Cu(3)–O(1)	1.913(9)	1.903(9)	1.912(13)	1.900(17)	Cu(5)–O(2)	1.914(10)	1.892(9)	1.908(14)	—
Cu(3)–O(1R)	1.970(10)	1.978(9)	1.988(14)	1.989(18)	Cu(5)–O(6R)	1.980(1)	1.980(8)	1.980(20)	—
Cu(3)–O(13A)	1.952(11)	1.942(9)	1.936(14)	1.976(18)	Cu(5)–O(21A)	1.938(11)	1.935(9)	1.940(20)	—
Cu(3)–N(7R)	1.996(12)	1.994(11)	1.953(11)	2.033(23)	Cu(5)–N(4R)	1.962(12)	1.999(11)	1.956(11)	—
Cu(4)–O(2)	1.865(10)	1.894(9)	1.902(14)	1.901(17)	Cu(6)–O(1)	1.893(9)	1.892(9)	1.917(13)	—
Cu(4)–O(3R)	1.963(10)	1.947(10)	1.967(14)	1.947(20)	Cu(6)–O(8R)	1.969(10)	1.959(8)	1.956(14)	—
Cu(4)–O(12A)	1.929(10)	1.930(9)	1.920(14)	1.951(22)	Cu(6)–O(14A)	1.952(11)	1.927(10)	1.954(14)	—
Cu(4)–N(2R)	2.020(11)	2.005(12)	1.964(12)	2.036(23)	Cu(6)–N(5R)	1.993(12)	2.010(12)	1.977(11)	—
Bonds involving coppers of [CuL$_4$] units									
Cu(7)–O(2R)	1.921(10)	1.938(9)	1.97(2)	1.949(21)	Cu(8)–O(4R)	1.944(10)	1.913(10)	1.95(2)	—
Cu(7)–O(7R)	1.923(10)	1.928(9)	1.98(2)	1.953(21)	Cu(8)–O(5R)	1.927(11)	1.908(10)	1.97(2)	—
Cu(7)–N(1R)	1.981(13)	1.975(12)	1.955(11)	1.988(24)	Cu(8)–N(6R)	2.003(13)	1.986(10)	1.942(11)	—
Cu(7)–N(3R)	1.978(12)	1.983(12)	1.953(11)	1.962(25)	Cu(8)–N(8R)	2.002(12)	1.984(10)	1.949(11)	—

[a] The Cu(1) and Cu(2) atoms lie on a crystallographic two-fold axis, therefore there are only three further crystallographically unique copper atoms in the molecule. [b] Symmetry equivalent to bond immediately above.

compounds (**4** and **4b**) the Cu–O bond lengths are considerably shorter than the Cu–N bonds, *e.g.* for **4** Cu–O averages 1.929 ± 0.015 Å while Cu–N averages 1.991 ± 0.013 Å. For **6** the difference is not statistically significant, but the Cu–O distances remain marginally shorter; for **5** the order is reversed, although again the difference is barely significant. The change appears to be due to the Cu–O bonds becoming longer as the substituent in the 6 position of the ligand is changed from Cl to Br to Me, which in turn can be related to the tautomerism of the pyridonate ligands. For strongly electron-withdrawing groups, *e.g.* Cl, the tautomerism of the protonated ligand lies toward the pyridin-2-ol form, *i.e.* the H atom would be attached to the oxygen rather than the ring nitrogen. For electron-releasing groups the pyridone form is favoured. Here the complex of the chp ligand has shorter M–O than M–N bonds, while for the mhp ligand the position is reversed.

Although the four octanuclear structures show considerable similarities at a molecular level, the packing of these molecules varies widely. This can be seen merely from the unit-cell dimensions for the four compounds. Of these the packing of **6**

Table 8 Bond angles (°) about copper in compounds **4**, **4b**, **5** and **6**

Compound	**4**	**4b**	**5**	**6***	Compound	**4**	**4b**	**5**	**6***
Angles involving copper atoms in shared edge of bitetrahedron									
O(1)–Cu(1)–O(24A)	97.1(4)	94.9(4)	96.0(6)	94.8(7)	O(1)–Cu(2)–O(2)	82.5(4)	83.9(4)	84.1(5)	83.3(7)
O(1)–Cu(1)–O(22A)	170.7(4)	171.4(4)	168.1(6)	168.7(8)	O(1)–Cu(2)–O(23A)	96.8(4)	95.4(4)	95.2(6)	95.3(7)
O(1)–Cu(1)–O(2)	82.4(4)	82.8(4)	83.9(5)	82.7(7)	O(1)–Cu(2)–O(11A)	168.9(4)	168.4(4)	168.1(6)	168.3(8)
O(24A)–Cu(1)–O(22A)	87.4(4)	89.1(4)	88.8(6)	89.8(7)	O(2)–Cu(2)–O(23A)	169.3(4)	170.7(4)	170.1(6)	168.3(8)
O(24A)–Cu(1)–O(2)	170.7(4)	170.0(4)	168.6(6)	168.7(8)	O(2)–Cu(2)–O(11A)	93.8(4)	94.5(4)	93.8(6)	95.3(7)
O(22A)–Cu(1)–O(2)	94.4(4)	94.5(4)	93.6(6)	94.8(7)	O(23A)–Cu(2)–O(11A)	88.7(4)	88.1(4)	88.8(6)	88.3(7)
O(1)–Cu(1)–O(1R)	75.8(4)	76.1(3)	77.3(5)	75.8(7)	O(1)–Cu(2)–O(8R)	74.9(4)	75.9(3)	76.7(5)	75.2(7)
O(24A)–Cu(1)–O(1R)	87.3(4)	90.1(3)	91.1(6)	89.4(7)	O(2)–Cu(2)–O(8R)	103.4(4)	100.9(3)	98.4(5)	100.5(7)
O(22A)–Cu(1)–O(1R)	96.6(4)	96.3(3)	91.8(6)	94.0(7)	O(23A)–Cu(2)–O(8R)	86.7(4)	87.8(3)	91.0(5)	90.3(7)
O(2)–Cu(1)–O(1R)	101.5(4)	98.7(3)	100.0(5)	100.6(7)	O(11A)–Cu(2)–O(8R)	96.0(4)	93.2(3)	92.1(5)	93.7(7)
O(1)–Cu(1)–O(6R)	94.7(4)	94.8(3)	97.8(6)	100.6(7)	O(3R)–Cu(2)–O(8R)	174.2(4)	176.6(3)	174.3(5)	174.5(8)
O(24A)–Cu(1)–O(6R)	93.7(4)	93.9(3)	91.2(6)	94.0(7)	O(11A)–Cu(2)–O(3R)	89.8(4)	89.3(4)	92.1(6)	90.3(7)
O(22A)–Cu(1)–O(6R)	93.0(4)	92.6(3)	92.9(6)	89.4(7)	O(1)–Cu(2)–O(3R)	99.3(4)	101.4(4)	98.8(5)	100.5(7)
O(2)–Cu(1)–O(6R)	77.1(4)	76.7(3)	77.6(5)	75.8(7)	O(2)–Cu(2)–O(3R)	75.4(4)	76.5(3)	77.4(5)	75.2(7)
O(1R)–Cu(1)–O(6R)	170.5(3)	170.4(3)	174.8(5)	175.2(8)	O(23A)–Cu(2)–O(3R)	94.2(4)	94.6(3)	93.0(6)	93.7(7)
Angles involving copper atoms at external vertices of bitetrahedron									
N(7R)–Cu(3)–O(13A)	86.6(5)	88.3(4)	92.0(6)	89.6(9)	N(4R)–Cu(5)–O(21A)	88.2(5)	88.9(4)	91.7(6)	—
N(7R)–Cu(3)–O(1R)	95.2(4)	94.8(4)	92.6(6)	93.3(9)	N(4R)–Cu(5)–O(6R)	93.5(5)	94.0(4)	92.3(6)	—
N(7R)–Cu(3)–O(1)	162.4(4)	163.8(4)	155.5(6)	164.5(10)	N(4R)–Cu(5)–O(2)	163.3(5)	161.8(4)	154.3(6)	—
O(13A)–Cu(3)–O(1R)	163.1(4)	163.9(4)	159.9(6)	161.3(10)	O(21A)–Cu(5)–O(6R)	167.4(4)	161.9(4)	158.1(6)	—
O(13A)–Cu(3)–O(1)	95.8(4)	93.6(4)	95.7(6)	94.4(9)	O(21A)–Cu(5)–O(2)	92.4(4)	93.7(4)	94.8(6)	—
O(1R)–Cu(3)–O(1)	87.6(4)	87.8(4)	88.1(6)	87.8(9)	O(6R)–Cu(5)–O(2)	89.5(4)	89.1(4)	90.8(6)	—
N(2R)–Cu(4)–O(12A)	88.9(4)	88.4(4)	93.0(6)	86.6(9)	N(5R)–Cu(6)–O(14A)	86.8(5)	89.3(5)	92.2(6)	—
N(2R)–Cu(4)–O(3R)	93.0(4)	92.9(4)	92.8(6)	96.0(9)	N(5R)–Cu(6)–O(8R)	94.4(5)	94.0(4)	91.9(5)	—
N(2R)–Cu(4)–O(2)	162.7(4)	159.7(4)	154.7(6)	164.8(9)	N(5R)–Cu(6)–O(1)	160.7(5)	158.8(4)	155.1(6)	—
O(12A)–Cu(4)–O(3R)	160.2(4)	161.7(4)	159.6(6)	165.8(9)	O(14A)–Cu(6)–O(8R)	164.8(4)	161.1(4)	160.5(6)	—
O(12A)–Cu(4)–O(2)	95.8(4)	95.6(4)	95.5(6)	93.6(9)	O(14A)–Cu(6)–O(1)	95.4(4)	95.3(4)	95.3(6)	—
O(3R)–Cu(4)–O(2)	88.2(4)	89.5(4)	87.5(6)	87.5(9)	O(8R)–Cu(6)–O(1)	88.5(4)	88.3(4)	88.6(6)	—
Angles involving copper atoms of [CuL_4] units									
N(1R)–Cu(7)–N(3R)	175.0(5)	174.8(5)	175.2(6)	175.1(10)	N(6R)–Cu(8)–N(8R)	174.2(5)	172.3(4)	173.8(7)	—
O(7R)–Cu(7)–O(2R)	173.0(4)	170.8(4)	169.8(7)	173.7(10)	O(4R)–Cu(8)–O(5R)	170.9(5)	168.7(4)	167.7(6)	—
N(1R)–Cu(7)–O(7R)	92.5(5)	94.3(4)	92.0(6)	94.0(10)	N(6R)–Cu(8)–O(4R)	91.6(5)	93.4(4)	92.3(6)	—
N(1R)–Cu(7)–O(2R)	86.7(5)	87.7(4)	88.4(6)	86.9(9)	N(6R)–Cu(8)–O(5R)	89.4(5)	87.6(4)	89.6(6)	—
N(3R)–Cu(7)–O(2R)	93.1(5)	92.2(4)	91.9(6)	94.4(10)	N(8R)–Cu(8)–O(4R)	87.4(5)	87.7(4)	88.3(6)	—
N(3R)–Cu(7)–O(7R)	88.3(5)	86.5(4)	88.6(6)	85.2(9)	N(8R)–Cu(8)–O(5R)	92.4(5)	92.8(4)	91.2(6)	—

* The Cu(1) and Cu(2) atoms lie on a crystallographic two-fold axis, therefore only three other crystallographically unique copper atoms are found.

Table 9 The Cu–Cu contacts (Å) and angles (°) at μ_4-oxo atoms within edge-sharing bitetrahedra in compounds **4**, **4b**, **5**, **6** and **11**

Compound	**4**	**4b**	**5**	**6**	**11**[a]
Contact in shared edge	2.955(2)	2.9327(25)	2.922(4)	2.923(4)	3.039(2)
Contact bridged by μ-O from L	3.065(2)–3.106(2)	3.051(2)–3.081(2)	3.044(4)–3.064(4)	3.084(5)–3.096(4)	3.167(2)–3.368(2)
Contact bridged by acetate	2.968(2)–3.035(2)	2.986(2)–3.056(2)	3.036(5)–3.055(5)	3.032(5)–3.043(4)	
Unbridged contact between external vertices within tetrahedra	3.489(2), 3.526(2)	3.490(3), 3.556(3)	3.554(4), 3.582(4)	3.483(5)	
Contact between external vertices in different tetrahedra	3.985(2), 4.069(2)	3.958(3), 4.055(3)	4.030(4), 3.954(4)	4.109(5)	4.466(2), 5.110(2)
Cu(1)–O(1)–Cu(2)	97.7(4)	97.4(4)	96.8(6)	97.0(8)	94.1(5)
Cu(1)–O(1)–Cu(3)	106.0(4)	105.7(4)	104.9(6)	106.8(8)	115.8(6)
Cu(1)–O(1)–Cu(6)	103.7(4)	105.0(4)	103.4(6)	103.6(8)	117.9(7)
Cu(2)–O(1)–Cu(3)	103.5(4)	103.2(4)	104.4(6)	104.6(8)	105.7(6)
Cu(2)–O(1)–Cu(6)	107.7(4)	106.2(4)	104.6(6)	106.6(8)	104.1(6)
Cu(3)–O(1)–Cu(6)	132.9(4)	133.7(4)	136.3(6)	132.8(8)	115.1(5)
Cu(1)–O(2)–Cu(2)	97.3(4)	95.9(4)	95.2(6)		89.7(4)
Cu(1)–O(2)–Cu(5)	104.7(4)	104.4(4)	103.3(6)		104.8(6)
Cu(1)–O(2)–Cu(4)	104.6(4)	102.7(4)	102.9(6)		102.0(5)
Cu(2)–O(2)–Cu(5)	99.5(4)	101.5(4)	103.3(6)		117.5(7)
Cu(2)–O(2)–Cu(4)	105.9(4)	104.5(4)	103.6(6)		117.7(6)
Cu(4)–O(2)–Cu(5)	137.9(4)	139.8(4)	140.2(6)		117.7(6)

[a] Data taken from ref 13. (Numbering scheme modified to conform with that used in this work. All inter-vertex contacts within the two tetrahedra are bridged.)

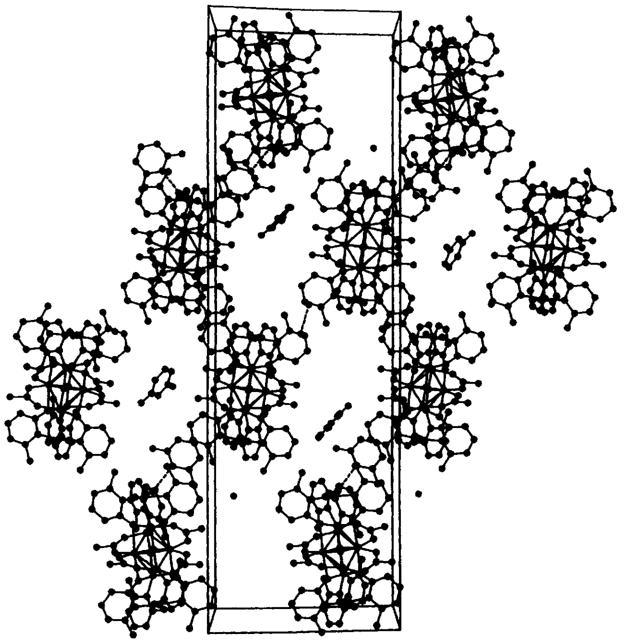

Fig. 2 The molecular packing of **5** viewed down the *a* axis, showing the large channels within the structure which are occupied by molecules of Hmhp

is perhaps the least interesting, with the octanuclear molecules adopting an essentially close-packed array.

The packing in **4**, **4b** and **5** all show a tendency for the formation of channels within the structure. This is most evident for **5** (Fig. 2) where the complex stacks parallel to the *a* axis, leaving channels within the crystal which are occupied by molecules of Hmhp and solvent. For **4** and **4b** the channels do not have such a large diameter, and are occupied by molecules of solvent, CH_2Cl_2 for **4** and acetone for **4b**. There are weak inter-molecular interactions in all the complexes. In **5** these are chiefly H bonds between the proton on the nitrogen of free Hmhp ligands and O atoms bound to Cu(7) within the complex (N ··· O 2.80 Å): in the other structures the nearest contacts are halide–halide, either involving solvent or directly between complexes. These interactions do not appear sufficient to explain the gross crystal-packing differences observed. This tends to indicate that there must be several possible crystalline phases for these large, asymmetric molecules. This is supported by the experimental observation that crystals of **5**, **6**, **7** and **8** do not survive cooling to 150 K.

Physical Studies.—Given the unusual octanuclear structure of these complexes we have undertaken a series of physical measurements. Unfortunately EPR spectroscopy was uninformative, with no signal observed for any of the compounds between 77 K and room temperature. Similarly electrochemical studies revealed no redox process for any of the compounds in any of the solvents tried (CH_2Cl_2, dimethylformamide or MeCN).

We have previously found that both **2** and $[Cu_7(mhp)_{12}][Pb(NO_3)_4]$ give excellent FAB mass spectral results,[16] therefore we hoped that the octanuclear complexes would also give interesting mass spectroscopic data. This has proved to be the case. Although we did not observe the molecular ion for any of the compounds, all gave a large number of peaks which could be assigned to sensible fragments of the parent. The complexity of the system means that several peaks could not be assigned unambiguously. The most interesting mass spectrum obtained is that of **6**, where peaks are seen for both $[Cu_7(O)_2(O_2CMe)_4(bhp)_8]$ ($M^+ - Cu$) and $[Cu_8(O)_2(O_2CMe)_4(bhp)_7]$ ($M^+ - bhp$), and a large number of polycopper fragments down to $[Cu_4(O)(O_2CMe)]$. Several peaks indicate loss of Br from the bhp ligand, which does not seem chemically unreasonable.

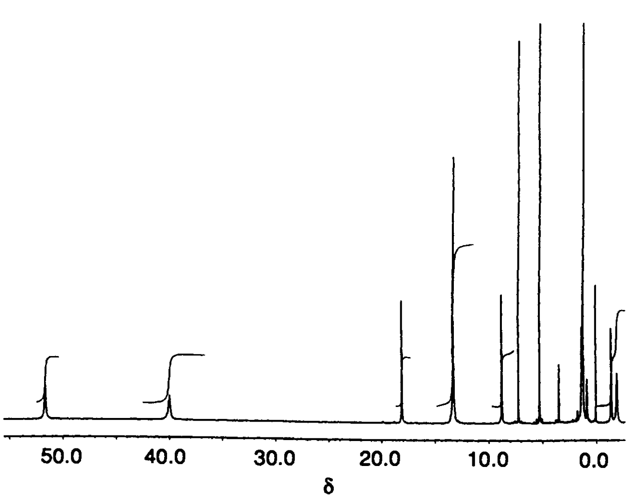

Fig. 3 The ^1H NMR spectrum of **4** showing the large chemical shift range

The NMR results are also interesting. Although all the compounds are paramagnetic those studied give well defined spectra spread over a chemical shift range δ 51 to −3 (Fig. 3). As each octanuclear complex contains two chemically inequivalent pyridonate ligands then six resonances of intensity one are expected due to these aromatic protons. In the acetate complexes one additional peak of intensity three is expected for the methyl group of the carboxylate, while in the benzoate complexes three peaks of intensities 2:2:1 are expected for the *ortho*, *meta* and *para* protons of the phenyl ring. Insufficient quantities of **4b** and **5** were obtained for NMR analysis.

The results are summarised in Table 10, which also includes data for **2**. As can be seen the chemical shifts of the octanuclear complexes are quite consistent, but differ from those in **2**. In particular, in **2** all resonances due to aromatic protons were found to have shifted to high frequency while in **4**, **6**, **7** and **8** two resonances due to aromatic protons are found with negative chemical shifts. Additionally the most positively shifted resonance in each of **4**, **6**, **7** and **8** is found at a considerably higher shift than the most shifted resonance in **2**. The complexity of the system, in which each ligand is attached to either two or three inequivalent copper atoms, prevents assignment of the resonances to specific pyridonate protons; it is also not possible to account for the direction and magnitudes of the chemical shifts in **2** and the octanuclear species. What is clear is that the NMR spectra are sufficiently well resolved to distinguish between species of different nuclearity, and species containing different carboxylate ligands. These spectra do not differentiate between the presence of the chp and bhp ligands.

Magnetic Studies.—There are many examples of magnetic exchange interactions in complexes containing tetrahedral Cu_4O cores.[44] Without exception the magnetic properties are dominated by antiferromagnetic exchange processes occurring through the μ_4-oxo bridge. Fig. 4 shows the variation of effective magnetic moment, μ_{eff}, with temperature for **4** and **6**. Above 100 K both complexes exhibit an effective magnetic moment considerably less than the 4.9 μ_B anticipated for eight non-interacting copper(II) ions. This is consistent with the antiferromagnetic coupling observed in other Cu_4O complexes.

The low temperature behaviour of the two materials diverges significantly. Compound **4** exhibits a steady increase in μ_{eff} below 75 K, whereas **6** exhibits a sharp decrease in μ_{eff} below 30 K. In order to explain this apparent anomaly in the behaviour of two structurally similar compounds we have developed

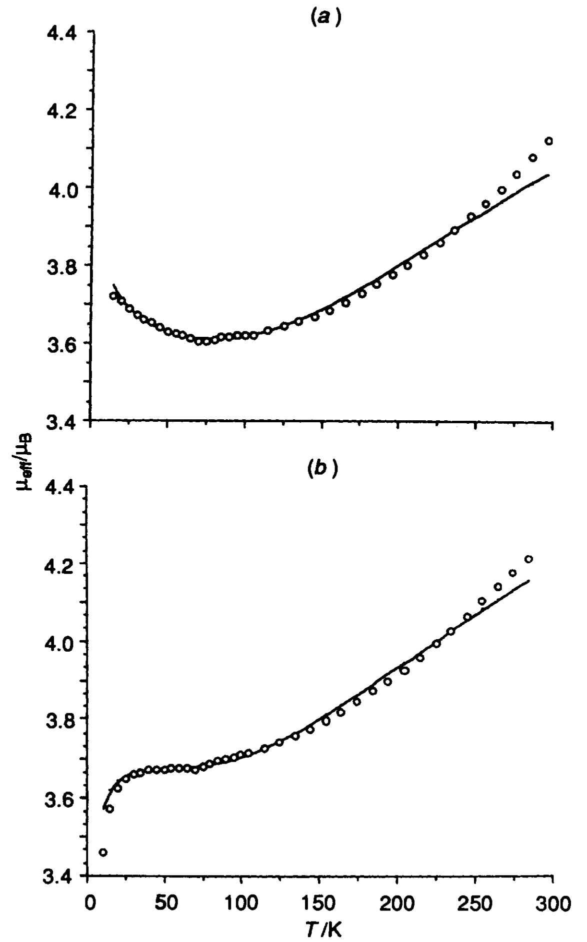

Fig. 4 Magnetic moment of **4** (*a*) and **6** (*b*) *vs.* temperature. Experimental data are shown as circles, and the full lines are simulations based on parameters given in the text

Table 10 The NMR results for copper–pyridonate complexes

	δ	
Compound	Aromatic H atoms of pyridonate ligands[a]	Carboxylate H atoms[b]
4	51.6, 39.9, 18.1, 8.8, −1.3, −1.9	13.3(3)
6	51.8, 40.2, 17.7, 8.1, −2.3, −2.5	13.4(3)
7	51.5, 40.0, 18.4, 8.6, −0.6, −1.1	8.8(2), 6.8(1), 5.2(2)
8	51.3, 40.0, 18.0, 7.8, −1.4, −1.7	8.8(2), 6.8(1), 5.0(2)
9	49.7, 41.8, 18.4, 9.5, 0.1, −0.8	*c*
2[d]	40.8, 40.4, 29.0, 22.0, 21.3, 18.3	*c*

[a] All resonances have relative intensity 1. [b] Relative intensities in parentheses. [c] Not applicable. [d] Data taken from ref. 16.

a model for the magnetic interactions in these species, concentrating on those interactions between copper atoms bridged by one or more of the μ_4-oxo bridges, *i.e.* Cu(1)–Cu(6). Since the terminal copper centres [Cu(7) and Cu(8)] possess neither short contacts to the central Cu_6O_2 core, nor a bridging ligand through which super-exchange can occur, we have modelled the system as a Cu_6O_2 core with two additional non-interacting spins.

Although the structure of the Cu_6O_2 core does not possess the highest possible symmetry, we have considered chemically similar environments to be magnetically equivalent. The interactions can be thought to be of three distinct types, all of which utilise one or more of the μ_4-O atoms. The structure of the Cu_6O_2 core, the exchange interactions and the atom labelling scheme are illustrated in Fig. 5. The three types of exchange interaction can be described as follows. First, there is exchange (exchange interaction parameter $= J_1$) between the copper ions at the centre of the core [Cu(1) and Cu(2)] and those at the extremities of the edge-shared bitetrahedron *i.e.* Cu(3), Cu(4), Cu(5) and Cu(6). There are eight such interactions, and each is bridged by one μ_4-O atom, plus either an acetate or pyridonate ligand. Secondly, there is exchange (J_2) between Cu(1) and Cu(2) at the shared edge of the bitetrahedron, with Cu(1) and Cu(2) bridged by both μ_4-O atoms. Thirdly, there are exchange interactions (J_3) between Cu(3) and Cu(6), and Cu(4) and Cu(5). Each of these edges are bridged by one μ_4-O atom but by no further ligand. We have neglected the final exchange terms [between Cu(3) and Cu(4), and Cu(5) and Cu(6)] because the Cu ⋯ Cu distance is large and there is no super-exchange pathway. The isotropic Heisenberg Hamiltonian for such a Cu_6O_2 core can then be written as in equation (1) where $\hat{S}_1$, $\hat{S}_2$, $\hat{S}_3$, $\hat{S}_4$, $\hat{S}_5$ and $\hat{S}_6$ are the spin operators for the copper centres Cu(1)–Cu(6) respectively. Following the vector-coupling method of Kambe,[45] we assign the following terms: $S_a = \hat{S}_1 + \hat{S}_2$, $S_b = \hat{S}_3 + \hat{S}_6$, $S_c = \hat{S}_4 + \hat{S}_5$, $S_d = S_b + S_c$ and $S_T = S_a + S_d$.

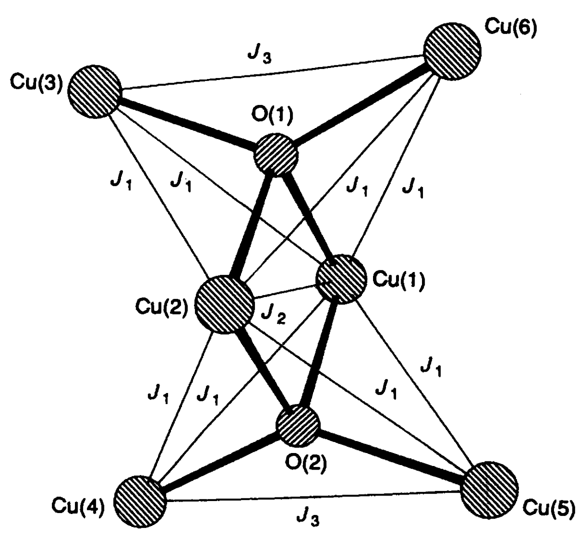

Fig. 5 The oxo-centred bitetrahedral core of **4** also showing the magnetic exchange interactions

$$\mathscr{H} = -2J_1(\hat{S}_1 + \hat{S}_2)(\hat{S}_3 + \hat{S}_4 + \hat{S}_5 + \hat{S}_6) - 2J_2\hat{S}_1\hat{S}_2 - 2J_3(\hat{S}_3\hat{S}_6 + \hat{S}_4\hat{S}_6) \quad (1)$$

Using these relationships, we can solve the Hamiltonian and determine the multiplicity and energy of each state. There are one septet, five quintet, nine triplet and five singlet states. The energy of each state is determined by equation (2). Substituting this energy term into the Van Vleck equation, we can derive the magnetic susceptibility of the Cu_6O_2 core (all terms have their usual meanings) [equation (3)]. Since we have assumed Cu(7)

$$E_{spin} = -J_1[S_T(S_T + 1) - S_a(S_a + 1) - S_d(S_d + 1)] - J_2[S_a(S_a + 1) - 2S(S + 1)] - J_3[S_b(S_b + 1) + S_c(S_c + 1) - 4S(S + 1)] \quad (2)$$

$$\chi_M = \frac{Ng^2\beta^2}{3kT} \frac{\sum S_T(S_T + 1)(2S_T + 1)\exp\left(-\frac{E_{spin}}{kT}\right)}{\sum (2S_T + 1)\exp\left(-\frac{E_{spin}}{kT}\right)} \quad (3)$$

and Cu(8) to be non-interacting, determination of the total magnetic susceptibility of the octanuclear complex becomes possible.

In order to minimise the number of variables in this equation, we undertook a study of the variation of magnetisation with applied magnetic field, from which we determined a mean *g* value. For $[Cu_8O_2(O_2CMe)_4(chp)_8]$ **4**, $g = 2.195$ and the three exchange terms were refined to $J_1 = -178(1)$, $J_2 = +68(1)$ and $J_3 = -183(1)$ cm^{-1}. For $[Cu_8O_2(O_2CMe)_4(bhp)_8]$ **6**, $g = 2.260$, $J_1 = -173(1)$, $J_2 = +73(1)$ and $J_3 = -170(1)$ cm^{-1}. The goodness-of-fit terms $(1 - \Delta)$* for $[Cu_8O_2(O_2CMe)_4(chp)_8]$ and $[Cu_8O_2(O_2CMe)_4(chp)_8]$ were 0.996 and 0.993 respectively. The experimental and calculated moments for both complexes are shown in Fig. 4.

Although both sets of parameters are reassuringly similar, and close to exchange interaction parameters reported for other oxo-centred Cu tetrahedra,[44] the observed response of μ_{eff} is different. Simulation shows that the low temperature behaviour of **4** and **6** is dependent on the relative magnitudes of J_1 and J_3. If J_1 is less negative than J_3 then we observe an increase in μ_{eff}; if $J_1 = J_3$ then μ_{eff} remains constant; and if J_1 is more negative than J_3 then μ_{eff} decreases. The term J_2 appears to have little influence in the low temperature region.

It has been shown[46] that the exchange interaction in Cu_2O_2 species, where the bridging O atoms are derived from hydroxide, is dependent on the mean Cu–O–Cu angle. If this angle is below 97.5° the exchange is predicted to be ferromagnetic. In **4** and **6** the mean angle at oxygen for the Cu(1)–O(1)–Cu(2)–O(2) ring is 97.5(4) and 97.0(8)° respectively. This is the Cu–Cu interaction for which the exchange parameter, J_2, is found to be ferromagnetic. The magnitude of this parameter is greater than that predicted on the basis of previous work,[46] however the magnetic behaviour of the complexes is little effected by moderate changes in J_2 and we suspect that this parameter is the least reliable of those we have calculated.

It is also worth noting that the angle at the bridging oxygen associated with J_3 is, at *ca.* 134°, comfortably the most obtuse angle in the system, and this probably explains why J_3 is so large despite the Cu–Cu vector being bridged by only one O atom, rather than the two O atoms which bridge the J_1 interaction. In seeking an explanation for the difference in the size of J_3 between **4** and **6** the different Cu–O–Cu angle, average 135° in **4**, 133° in **6**, may be significant; however magnetostructural correlations which apply to simple dimeric species may not necessarily hold for more complicated structures where additional super-exchange pathways may operate.

Conclusion

The octanuclear copper(II) complexes reported here represent a further addition to the limited number of pyridonate complexes of the first transition series. The structures are interesting, featuring a bitetrahedral arrangement of copper atoms, and, along with the dodecanuclear cobalt complex characterised by Clegg *et al.*,[42] suggest that the use of a combination of carboxylate and pyridonate ligands might be a route to high nuclearity assemblies of 3d metals. Recently our isolation and structural characterisation of a cyclic assembly, $[Ni_{12}(O_2CMe)_{12}(chp)_{12}(H_2O)_6(thf)_6]$[47] (thf = tetrahydrofuran), tends to confirm this supposition.

Characterisation of such assemblies continues to be problematic and utterly reliant on X-ray crystallography. The results reported here indicate that FAB mass and NMR spectra of these complexes can be highly informative. For example, it is possible to predict the structures of the complexes containing benzoate and trifluoroacetate groups by comparing their NMR spectra with those of the acetate complexes. The formula of **6** is almost predictable from analytical data and FAB mass spectra. It remains true, however, that without a crystal structure determination of at least one member of a series even determining the stoichiometry of the products would be extremely difficult and never absolutely unambiguous.

The magnetic data reported illustrate the delicate balance that can occur in spin-frustrated systems. The difference between the response of **4** and **6** is caused by a change of *ca.* 10 cm^{-1} in the magnitude of one exchange coupling. This in turn may be related to a 2° change in a bond angle at a bridging ligand. Such subtle changes are both exciting, in that they demonstrate the degree to which magnetic properties can be altered by seemingly trivial changes in structure, and challenging, in that such changes can presently be neither predicted nor fully controlled. Much more work in the area of synthesis, structural characterisation and study of polynuclear complexes is necessary to allow the design of species with specific, desirable magnetic properties.

Acknowledgements

We are grateful to the SERC for a studentship (to C. M. G.), a post-doctoral fellowship (to S. P.) and for funding for a diffractometer and SQUID susceptometer, and to the Leverhulme Trust for a post-doctoral fellowship (to J. M. R.). We also thank Drs. C. K. Prout and D. J. Watkin of the University of Oxford for X-ray data collection for compound **5**, Mr. S. E. Lawrence of the University of Durham for the DSC data and Dr. V. A. Cherepanov of the Ural State University, Russia for the TGA data.

References

1 See, for example, D. Fenske and W. Holstein, *Angew. Chem., Int. Ed. Engl.*, 1994, **33**, 1290 and refs. therein.
2 J. R. Carruthers, C. K. Prout and F. J. C. Rossotti, *Acta Crystallogr., Sect. B.*, 1975, **31**, 2044.
3 M. Ahlgren, U. Turpeinen and K. Smolander, *Acta Crystallogr., Sect. B.*, 1980, **36**, 1091.
4 R. J. Butcher, C. J. O'Connor and E. Sinn, *Inorg. Chem.*, 1981, **20**, 537.
5 R. J. Butcher, J. W. Overman and E. Sinn, *J. Am. Chem. Soc.*, 1980, **102**, 3276.
6 K. Smolander, *Acta Chem. Scand., Ser. A.*, 1983, **37**, 5.
7 Z. Olejnik, B. Jezowska-Trzebiatowska and T. Lis, *J. Chem. Soc., Dalton Trans.*, 1986, 97.
8 H. Muhonen, W. E. Hatfield and J. H. Helms, *Inorg. Chem.*, 1986, **25**, 800.
9 N. A. Bailey, D. E. Fenton, R. Moody, P. J. Scrimshire, E. Beloritzky, P. H. Fries and J.-M. Latour, *J. Chem. Soc., Dalton Trans.*, 1988, 2817.
10 U. Turpeinen, R. Hämäläinen and J. Reedijk, *Inorg. Chim. Acta*, 1988, **154**, 201.
11 B. F. Hoskins, R. Robson and P. Smith, *J. Chem. Soc., Chem. Commun.*, 1990, 488.
12 K. D. Karlin, Q.-F. Gan, A. Farooq, S. Liu and J. Zubieta, *Inorg. Chem.*, 1990, **29**, 2549.
13 Y. Agnus, R. Louis, B. Metz, C. Boudon, J. P. Gisselbrecht and M. Gross, *Inorg. Chem.*, 1991, **30**, 3155.
14 V. A. Igonin, O. I. Shchegolikhina, S. V. Lindeman, M. M. Levitsky, Y. T. Struchkov and A. A. Zhdanov, *J. Organomet. Chem.*, 1992, **423**, 351.
15 A. J. Blake, R. O. Gould, P. E. Y. Milne and R. E. P. Winpenny, *J. Chem. Soc., Chem. Commun.*, 1991, 1453.
16 A. J. Blake, R. O. Gould, C. M. Grant, P. E. Y. Milne, D. Reed and R. E. P. Winpenny, *Angew. Chem., Int. Ed. Engl.*, 1994, **33**, 195.
17 J. A. Real, G. De Munno, R. Chiapetta, M. Julve, F. Lloret, Y. Journaux, J.-C. Colin and G. Blondin, *Angew. Chem., Int. Ed. Engl.*, 1994, **33**, 1184.
18 E. Agostinelli, D. B. Dell'Amico, F. Calderazzo, D. Fiorani and G. Pelizzi, *Gazz. Chim. Ital.*, 1988, **118**, 729.
19 V. McKee and S. S. Tandon, *J. Chem. Soc., Dalton Trans.*, 1991, 221.
20 G. A. Ardizzoia, M. A. Angaroni, G. La Monica, F. Cariati, S. Cenini, M. Moret and N. Masciocchi, *Inorg. Chem.*, 1991, **30**, 4347.

---

* Refinement was carried out by minimising the term $D = (1/n) \times \Sigma|\chi_{obs} - \chi_{calc}|/\chi_{obs}$, where n is the number of data points and χ_{obs} and χ_{calc} are the observed and calculated molar magnetic susceptibilities respectively.

21 S. Wang, S. J. Trepanier and M. J. Wagner, *Inorg. Chem.*, 1993, **32**, 833.

22 W. H. Watson and W. W. Holley, *Croat. Chem. Acta*, 1984, **57**, 467.

23 U. Turpeinen, R. Hämäläinen and J. Reedijk, *Inorg. Chim. Acta*, 1987, **134**, 87.

24 R. E. Norman, N. J. Rose and R. E. Stenkamp, *J. Chem. Soc., Dalton Trans.*, 1987, 2905.

25 S. S. Tandon, L. K. Thompson and J. N. Bridson, *J. Chem. Soc., Chem. Commun.*, 1992, 911.

26 A. J. Blake, R. O. Gould, P. E. Y. Milne and R. E. P. Winpenny, *J. Chem. Soc., Chem. Commun.*, 1992, 522.

27 A. J. Blake, C. M. Grant, P. E. Y. Milne, J. M. Rawson and R. E. P. Winpenny, *J. Chem. Soc., Chem. Commun.*, 1994, 169.

28 A. J. Blake, C. M. Grant, J. M. Rawson and R. E. P. Winpenny, unpublished work.

29 G. R. Newkome, J. Broussard, S. K. Staires and J. D. Sauer, *Synthesis*, 1974, 707.

30 J. M. Rawson, University of Durham, 1990.

31 A. J. Blake, R. O. Gould and R. E. P. Winpenny, *Acta Crystallogr., Sect. C*, 1991, **47**, 1077.

32 G. M. Sheldrick, SHELX 76, University of Cambridge, 1976.

33 G. M. Sheldrick, SHELXL 93, University of Göttingen, 1993.

34 J. Cosier and A. M. Glazer, *J. Appl. Crystallogr.*, 1986, **19**, 105.

35 W. Clegg, *Acta Crystallogr., Sect. A*, 1981, **37**, 22.

36 A. C. T. North, D. C. Phillips and F. S. Matthews, *Acta Crystallogr., Sect. A*, 1968, **24**, 351.

37 G. M. Sheldrick, SHELXS 86, University of Göttingen, 1986.

38 P. T. Beurskens, W. P. Bosman, H. M. Doesburg, R. O. Gould, Th. E. M. Van den Hark, P. A. J. Prick, J. H. Noordik, G. Beurskens, V. Parthasarathi, H. J. Bruins-Slot, R. C. Haltiwanger, M. K. Strumpel and J. M. M. Smits, *Crystallographic Computing 3*, eds. G. M. Sheldrick, C. Krüger and R. Goddard, Clarendon Press, Oxford, 1985, pp. 216–226.

39 C. J. O'Connor, *Prog. Inorg. Chem.*, 1982, **29**, 203.

40 *Handbook of Chemistry & Physics*, ed. R. C. Weest, CRC Press Inc., Boca Raton, FL, 70th edn., pp. E134.

41 J. M. Rawson, University of Edinburgh, 1994.

42 W. Clegg, C. D. Garner and M. H. Al-Samman, *Inorg. Chem.*, 1983, **22**, 1534.

43 C. M. Grant, unpublished work.

44 S. Teipel, K. Grieser, W. Haase and B. Krebs, *Inorg. Chem.*, 1994, **33**, 456 and refs. therein.

45 K. Kambe, *J. Phys. Soc. Jpn.*, 1950, **5**, 48.

46 V. H. Crawford, H. W. Richardson, J. R. Wasson, D. J. Hodgson and W. E. Hatfield, *Inorg. Chem.*, 1976, **15**, 2107; D. J. Hodgson, *Prog. Inorg. Chem.*, 1975, **19**, 173.

47 A. J. Blake, C. M. Grant, S. Parsons, J. M. Rawson and R. E. P. Winpenny, *J. Chem. Soc., Chem. Commun.*, 1994, 2363.

Received 3rd *August* 1994; *Paper* 4/04766D